Microgrid Resilience Enhancement with Sensor Network-Based Monitoring and Risk Assessment Involving Uncertain Data

Tangxiao Yuan, Kossigan R. Assilevi, Kondo Hloindo Adjallah, Ayité S.A. Ajavon, Huifen Wang

energies

MDPI

Article

Microgrid Resilience Enhancement with Sensor Network-Based Monitoring and Risk Assessment Involving Uncertain Data

Tangxiao Yuan [1,2,*], Kossigan Roland Assilevi [3,*], Kondo Hloindo Adjallah [2,3], Ayité Sénah A. Ajavon [3] and Huifen Wang [1]

[1] School of Mechanical Engineering, Nanjing University of Science and Technology, Nanjing 210094, China; wanghf@njust.edu.cn
[2] LCOMS, Université de Lorraine, 57070 Metz, France; kondo.adjallah@univ-lorraine.fr
[3] Centre d'Excellence Régional pour la Maîtrise de l'Electricité (CERME), Université de Lomé, Lomé 01 BP 1515, Togo; asajavon@yahoo.fr
* Correspondence: yuantx@njust.edu.cn (T.Y.); roland.assilevi@cerme-togo.org (K.R.A.)

Abstract: This paper focuses on enhancing the resilience of microgrids—localized power systems that integrate multiple energy sources—against challenges such as natural disasters, technological obstacles, and human errors. It begins by defining the specific connotation of microgrid resilience and then proposes an innovative solution centered on the use of advanced sensor technology to continuously monitor the microgrid and its operational environment, ensuring accurate and timely data collection under dynamic conditions. Subsequently, a decision risk assessment framework is constructed, integrating data quality evaluation and operational risk considerations, to drive strategy optimization through in-depth data analysis. At the application level, this framework is successfully applied to two critical decision-making scenarios: the first is to optimize the power allocation strategy between solar energy and the auxiliary grid, aiming to maximize cost efficiency and minimize power outage losses; the second is to develop low-risk maintenance plans based on the predicted failure probabilities of microgrid components with uncertain information. Both decision processes skillfully utilize Monte Carlo simulation and multi-objective genetic algorithms to effectively manage the uncertainty risks in the decision-making process, thereby significantly enhancing the overall resilience of the microgrid.

Keywords: microgrid; resilience; sensor network; risk; decision making

Citation: Yuan, T.; Assilevi, K.R.; Adjallah, K.H.; Ajavon, A.S.A.; Wang, H. Microgrid Resilience Enhancement with Sensor Network-Based Monitoring and Risk Assessment Involving Uncertain Data. *Energies* **2024**, *17*, 6141. https://doi.org/10.3390/en17236141

Academic Editor: Tek Tjing Lie

Received: 17 October 2024
Revised: 17 November 2024
Accepted: 28 November 2024
Published: 5 December 2024

1. Introduction

The resilience of microgrids facing natural disaster scenarios can be enhanced through sensor network-based monitoring and a risk-based management decision approach. This involves deploying advanced sensor technologies to continuously monitor the microgrid and its environment, ensuring the accuracy and reliability of the data collected during natural disasters. By integrating risk assessment tools, the current study seeks to identify microgrids' potential vulnerabilities in natural disaster situations and predict the impact of information uncertainties on microgrid operation decisions for quick recovery. This approach requires the development of adaptive and right decision strategies that can promptly consider data quality influences due to uncertainties, ensuring the stable and efficient operation of microgrids after natural disasters to maintain a continuous power supply.

1.1. Microgrids

In an architectural paradigm, a microgrid incorporates several energy sources connected to different devices, such as power converters, storage batteries, power transportation and distribution lines, power management devices (inverters, switches, and regulators), and a supervision and management system. Figure 1 depicts a microgrid architecture, in diagram form, and highlights its various basic components, including generators (wind

turbines, photovoltaic (PV) panels, fuel cells, diesel engines, etc.), storage batteries, supercapacitors, flywheels, converters, switching devices, power transportation buses, and loads. Microgrids can be dedicated to direct-current (DC), alternating-current (AC), or hybrid (AC/DC) electric power supply [1]. Bus implementation depends on the power consumed at the load level. In general, DC microgrids are sufficient to provide power to common small loads of a few kW. AC microgrids consist of one or more AC buses connected to an AC load through AC interface components. DC/AC power electronic interface devices enable the powering of AC loads from batteries and photovoltaic panels. The AC supply enables the use of existing equipment, while the DC supply enables the use of some simple converters [2]. Hybrid AC/DC microgrid interconnect AC and DC microgrids through a bidirectional AC/DC converter to take advantage of both AC and DC power supply. Such microgrids can reliably connect directly to an auxiliary grid for power procurement in crises.

A microgrid can operate in standalone mode or be connected to a main or an auxiliary grid. Various control schemes, from basic control such as centralized, decentralized, and distributed control to multi-level control such as hierarchical control, can be applied to microgrids [3,4].

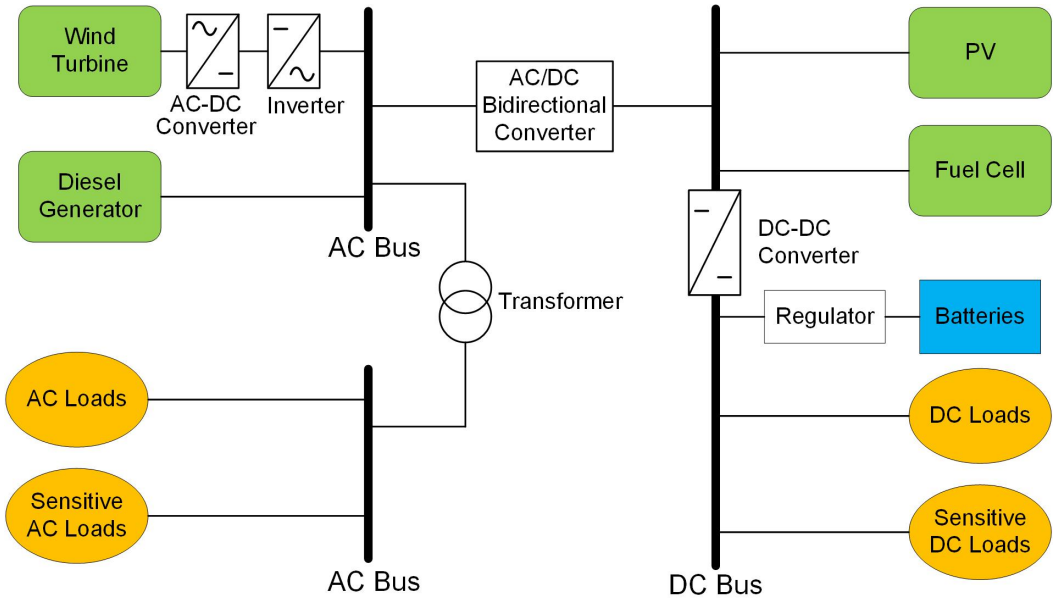

Figure 1. Microgrid general architecture.

Microgrids are susceptible to damage, performance hindrance, and substantial losses due to external events like natural catastrophes, technological malfunctions, human error, or criminal actions. So, microgrids' resilience needs to be considered from the very beginning of their design, since they require high operational availability to face such events [5,6]. Hence, it is crucial to identify potential vulnerabilities and threats and assess corresponding risks to develop and implement appropriate strategies for ensuring microgrid resilience.

1.2. Microgrid Condition Monitoring

Microgrid resilience consists in, after a disruptive event (key equipment failure, damages due to natural disaster, human error, or malicious action), restoring the microgrid to safe operational conditions quickly, starting from the critical situation, through suitable actions while relying on relevant information and right decisions, which may be challenging [7,8].

To establish a robust basis for decision making, it is essential to rely on data from the intrinsic behavior of the microgrid, as well as from its environment, including interactions with human operators. For this purpose, one can implement sensor network technologies

to collect data, monitor the microgrid system, assess the risks, and then optimize resilience decisions.

Sensor networks are relevant to monitor power microgrids and collect data to derive information useful for safety integrity and associated risk reduction. Assuming an optimal architecture sensor network, we are interested in its implementation in lossless data collection for risk anticipation and resilience in renewable energy source power microgrids [9–11]. The sensors must be placed at optimal positions to collect data relevant to assessing the risks, making the right decisions, and thus controlling microgrid resilience.

Thus, one can upgrade the microgrid architecture, in Figure 1, for instance, with sensors optimally networked through transceivers, using the microgrid power transmission line structure, as depicted in Figure 2, to transfer the data, and monitor and predict event risks quickly. The sensor network can also monitor the power flow (current and voltage), to detect transmission line failures (voltage drop, short-circuit, current leakage, line breakage, source outage, etc.).

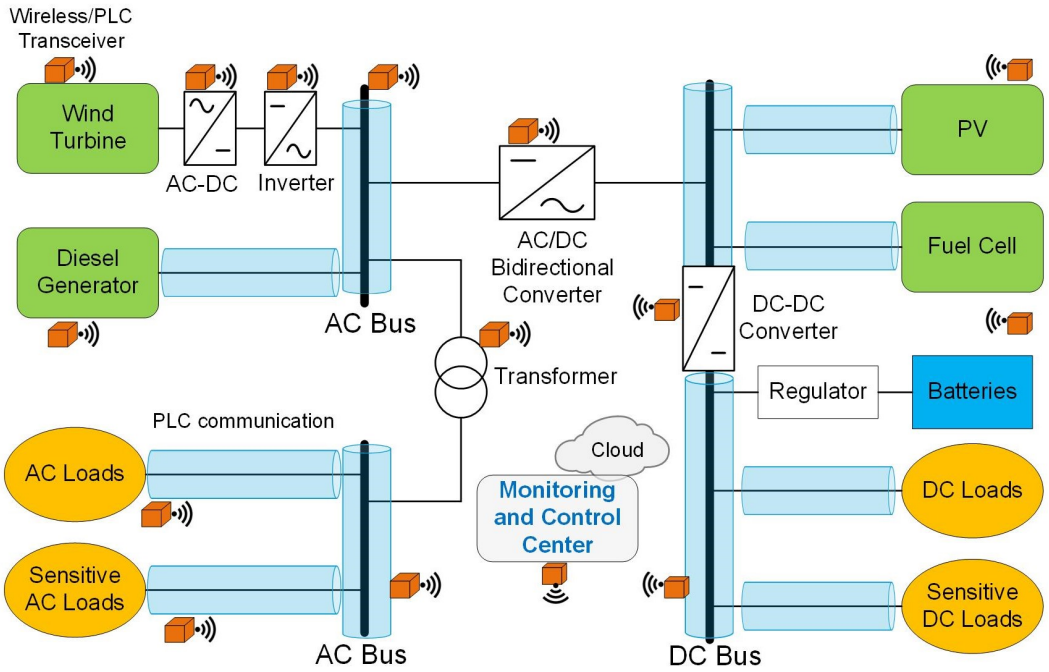

Figure 2. Microgrid architecture with sensor network.

1.3. Risk-Based Condition Monitoring

The previous subsection highlighted the importance of monitoring the microgrid system by using a smart sensor network. However, monitoring the intrinsic state of the microgrid alone is insufficient for risk-based resilience control. Risk assessment is a complex process that involves interactions in space and time between the event itself and the potential consequences [12].

Therefore, working out a microgrid resilience control strategy that considers risk factors requires monitoring the microgrid's intrinsic and external operating conditions, including interactions with human operators. Condition monitoring implies collecting condition data in real time from various sources, including human interactions, machines, and objects, using smart sensors, cameras, wireless networks, power line communications (PLCs), and various other technologies. Current and historical data allow for the prediction of microgrid system behavior. Some prediction information, such as weather forecasts or patterns of specific loads, can stem from external service platforms.

2. Resilience Process in Microgrids

Let us recall that the resilience of a system is an internal process within the latter, which allows it to restore its balance (of the microgrid energy flow) and initial performance stability after having been subjected to an unforeseen extreme event that has disrupted its internal structure as well as its vital functions.

The issue of resilience is addressed from several perspectives and modeled along four dimensions: objectives and measures, scenarios, control methods, and strategies [13]. Resilience is also addressed through the systematic evaluation of responses to potential threats following the identification of microgrid vulnerabilities and the implementation of developed mitigation strategies [14]. The authors in [15] present a comprehensive and up-to-date review of the literature on two broad categories of approaches to improving the resilience of microgrids in electricity distribution: optimal microgrid system design and operations planning, and energy management. Resilience is the ability to anticipate, resist, bounce back from, and adapt to sudden, unforeseen, and unprecedented disruption. The disruptions here refer to events designated as High Impact Low Probability (HILP) [16].

The synergetic process, from system failure to total recovery, corresponds to the resilience process. This process includes the times for inspection, fault detection, diagnosis, intervention means preparation, failure fixing, and gradual system restoration with the coordination of various actions. As shown in Figure 3, there are three types of resilience progress. In the figure, the red curve illustrates the resilience process of a microgrid system without specific monitoring and coordinated actions. At time t_1, due to external disastrous events or to the system's internal components' age, wearing, or degradation, certain components fail, which makes the system's resilient performance drop to level L_1 with an almost infinite degradation rate. During the time from t_1 to t_5, maintenance engineers analyze available information and diagnose the faults, decide on inspections by qualified personnel, and identify the failed components before the repair crews prepare spare parts and tools, some of which may need to be purchased separately, and go on site for interventions. From t_5 to t_6, the repair crews implement tools and parts at the repair site. The repair activities are then carried out step by step; thus, the system gradually recovers to its initial state.

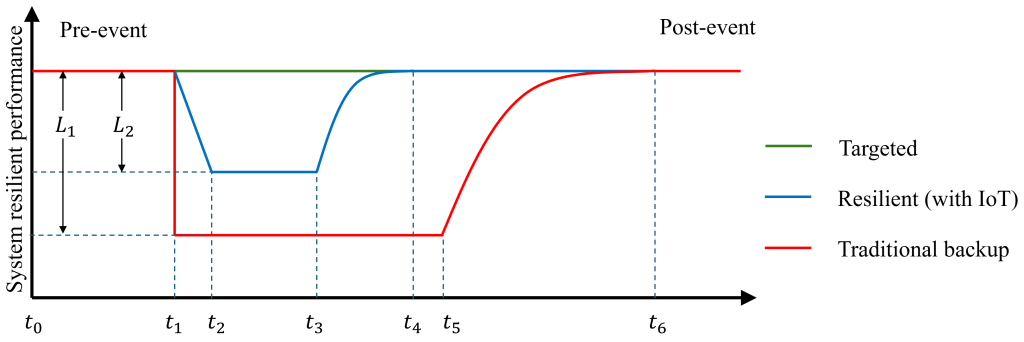

Figure 3. Microgrid resilience progress with IoT.

The blue curve in Figure 3 illustrates the resilience process relying on IoT technology. At time t_1, when aging and wearing components cause system failures subject to the effects of external disastrous unforeseen events, IoT technology enables the rapid uploading of component status information to the monitoring system. The latter triggers inspections and helps to make decisions quickly. By time t_2, system resilient performance declines up to $L_2 > L_1$, at a lower degradation rate because early detection allows for quick repair interventions. The low degradation rate from t_1 to t_2 relates to better microgrid withstanding against the effects of unforeseen disastrous events. During the period from t_2 to t_3, IoT technology allows for inspections to quickly locate fault points, significantly shortening the fault diagnosis time. Additionally, the procurement of spare parts can be anticipated to further reduce logistic time for failed-component replacements through fault

prediction. From t_3 to t_4, information provided by the IoT also helps optimize the schedule of maintenance tasks, further shortening the overall repair time in multi-fault scenarios.

The dark green curve in Figure 3 illustrates the resilience process when both the internal and external environments of the microgrid are predictable. When the impact on the internal system can be predicted, proactive maintenance can be carried out, and key components that are about to degrade or fail can be replaced, thus preventing unexpected system shutdowns. Furthermore, by predicting the microgrid's load power consumption and power generation capacity, the risk of system downtime can be reduced through the efficient use of electric power.

To initiate this process, the system must have up-to-date information on its state and recognize its critical situation. It can then implement its self-organization and feedback functions through appropriate decisions by exploiting information from historical and real-time data. It, therefore, emerges from this analysis that the availability and quality of data are essential to the key components of the resilience process, including information, self-organization, and feedback decisions to regain balance and stability. So, the term resilience control will be used in the rest of the paper to denote the resilience decision-making process.

Our concern in this paper relates peculiarly to the reliability problems of the information used in the resilience decision-making process and the reduction in associated risks. More specifically, this paper focuses on the evaluation of decision risks stemming from data collection, data uncertainties, their real-time impacts, and possible mitigation through the real-time improvement in the data collection process. In this work, the self-organization decisions include power sources and load reconfiguration. Additionally, the feedback decisions involve all actions defined in real-time automatic control or pre-defined maintainability solutions and real-time maintenance actions with integrated logistics.

2.1. Difference Between Power System Resilience and Microgrid Resilience

Power system resilience and microgrid resilience are defined essentially in the same way, sharing a foundational concept: both refer to the ability to withstand and recover from abnormal or disruptive conditions and both referring to the ability to recover under abnormal conditions. However, due to different application contexts, they exhibit significant differences in terms of scale, control objectives, and technical approaches.

The study of power system resilience has a long history, primarily focusing on power distribution and transmission systems within national or regional power grids [17]. Its control aims to maintain the overall stability and availability of the power system. Control targets often include substations, transmission lines, and power plants, with primary techniques focused on redistributing and dispatching power to respond to large-scale disturbances and restore system operation. In contrast, the scope of microgrid resilience is more localized, with a focus on ensuring that the microgrid can respond and recover rapidly in a short time frame, while relying more on local energy storage and renewable energy resources. Its control targets include equipment and components with mutual compensation among various renewable energy sources. The technical approaches adopted are generally simpler and more flexible, aiming to enable efficient local resource scheduling and self-sufficient power supply.

To summarize, while both concepts fundamentally involve recovery under abnormal conditions, in practical applications, power system resilience focuses on overall stability at the macro level, whereas microgrid resilience emphasizes rapid response and the optimization of local resources.

2.2. Risk-Based Predictive Maintenance

Risk-based predictive maintenance (RBPM) improves microgrid resilience by proactively identifying failure risks and prioritizing maintenance actions according to risk severity [18]. RBPM uses real-time data and predictive analytics to assist in preventing unexpected breakdowns and optimize maintenance plans. Such a proactive strategy guaran-

tees that high-risk components are addressed before they fail, reducing system disruptions and assuring continued operation, even during extreme events [19].

A risk-based maintenance policy enables microgrids to efficiently allocate resources by focusing on the most essential components, resulting in less total system downtime. Furthermore, RBPM reduces hazards during maintenance activities, ensuring that repairs are completed at the ideal time to avoid further issues. Microgrids can swiftly recover from outages by optimizing the processing time of scheduling and maintenance activities, thus increasing the microgrid dependability and operational efficiency [20–22].

Risk-based predictive maintenance increases resource use and component lifespan by forecasting failure rates and scheduling maintenance tasks at the optimal moment. Faster recovery from maintenance activities, particularly in crisis-prone contexts, guarantees that microgrids continue power delivery while minimizing performance loss. Overall, RBPM enhances microgrid resilience by minimizing the total risk of failure, improving dependability, and guaranteeing that important systems remain operational when stressed.

2.3. Issues of Information Uncertainty

In this subsection, we examined the requirements of the condition and the environmental monitoring of microgrids, pointing out their importance in resilience control decision support under uncertainty. However, data used to make decisions are subject to the challenging issue of data quality due to failures of sensors and communication networks, electronic or electromagnetic disturbances of data acquisition devices, etc. Although data quality may be improved in preprocessing, uncertainties cannot be ignored. The quantitative values of risks are assessed from the collected data and are very close to zero in the interval $[0, 1]$, so they are very sensitive to uncertainties and must be fairly complete and precise.

In traditional monitoring scenarios, data involving faulty sensors and human errors may lead to making a wrong decision.

Unlike the above situations, when data are used for decision making in a real-time control process, uncertainties may be amplified in the decision-making chain with wrong-decision risk propagation [23].

Hence, in the case of microgrids, ensuring high data quality is essential. During real-time data collection and transmission, data quality requirements are manifold and include accuracy, timeliness, completeness, consistency, security, and reliability.

Accuracy refers to the correctness and error-free nature of the data, which can be compromised by sensor malfunctions such as frozen states, bias, drift, and degraded precision [24]. Timeliness expresses how quickly data are refreshed and made available for decision making; data transmission network malfunctions and cyber-attacks can affect this requirement [25]. Completeness ensures that all necessary data points are available and accounted for in decision making. Consistency ensures that the data are normalized across different sources and over time [24]. Security involves protecting the data from unauthorized access and tampering, while reliability ensures that the data are dependable and can be accessed for decision making.

3. Risk Assessment-Based Decision Support Involving Uncertain Data

3.1. Framework of Decision Risk Assessment

This section introduces a framework of decision risk assessment and resilience control in microgrid systems, as illustrated by the comprehensive diagram in Figure 4. The framework allows for managing decision risks and controlling the resilience of a microgrid system through a data-driven approach.

The process begins with the collection of data from various sources, including design, tests, operations, digital twin, the microgrid, human interactions of the microgrid, and its influential environment. The collected data are stored in raw databases first.

Next, data are preprocessed to ensure their accuracy and enhance their quality. Data preprocessing includes detecting and removing outliers, replacing missing data with re-

liable estimations, correcting erroneous data, and validating the information extracted. The database is then updated with high-quality reliable data so that it can be used for subsequent analyses.

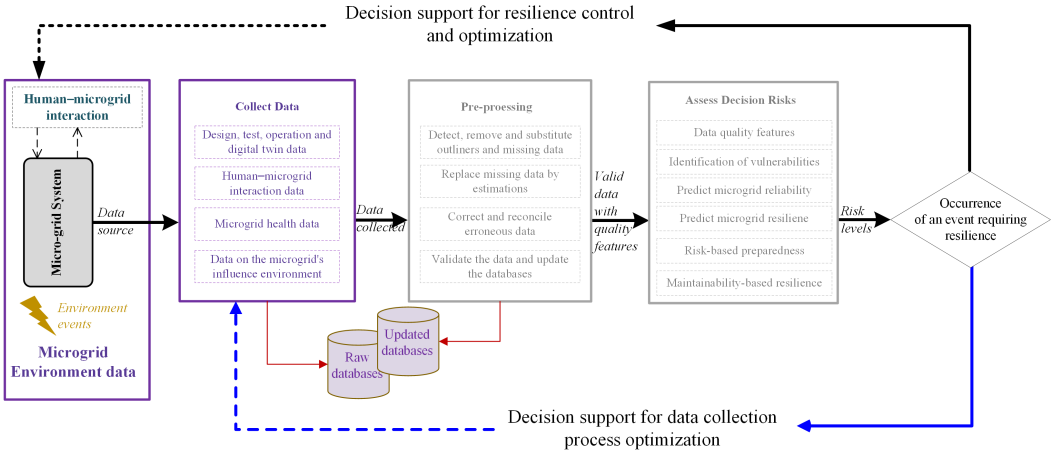

Figure 4. Data-driven decision risk assessment and resilience control process for microgrid.

Then, the diagram outlines the risk assessment phase, where decision risks are evaluated by considering factors such as data quality, vulnerabilities, operation hazards, failure risks, and microgrid resilience. These assessments yield the risk levels in the microgrid system.

Lastly, one determines the need to initiate resilience actions after the occurrence of a critical event. If this is the case, appropriate resilience measures are triggered. Otherwise, data collection and decision-making processes are further optimized, so as to ensure the continuous reduction in resilience factors.

The final step in the framework of decision risk assessment and resilience control focuses on evaluating the risk of the current decision in the presence of uncertain data. Assuming decision models, Algorithm 1 illustrates the specific steps in the decision-risk assessment.

3.2. Decision Making in Microgrids

In the context of microgrid resilience, the reliability and availability of data and information are the priority, as these are essential for informed decision making, particularly concerning management and historical data in manufacturing systems, preventing accident losses due to an extreme event through risk-based predictive maintenance techniques [26]. Building on this, accurately scheduling decisions of predictive maintenance while relying on components' health monitoring data is crucial to avoiding early or delayed interventions, which can help reduce the risk of failures during extreme events. Effective management decisions should also aim at preventing waste or losses of produced electric power by optimal resource use. Finally, with these risks managed, emergency decisions such as islanding operations can be made safely and promptly to ensure the resilience of the grid, while ensuring smooth maintenance interventions.

We consider in this article the three following categories of decisions for microgrid resilience, as Figure 5 shows: (1) real-time power flow control, (2) restoring the microgrid to the operational condition, and (3) proactive control and predictive maintenance.

3.2.1. Real-Time Energy Flow Control Decisions

Real-time energy flow control decisions mainly focus on power generation, energy storage, and load management within the microgrid and on the system's stable operation. In power generation, the power output of solar panels, wind turbines, and diesel generators is monitored, controlled, and scheduled online in real time according to the load demand and power generation capacity. At the same time, clean renewable energy power

generation, involving, for instance, solar energy and wind energy, with better economic and environmental impact is given priority to supply critical loads. This implies temporarily delaying non-critical loads if necessary.

Algorithm 1 : Risk assessment for decision with uncertain information.

Step 1: Make a decision based on current information and decision model
Input: Current Information, Decision Model
Output: One Decision
Decision = Decision_Model(Information)
Step 2: Identify risks using expert knowledge and build a risk assessment model
Input: Expert Knowledge, Current Scenario
Output: Risk Assessment Model (Model_r)
r = Identify_Risks(Expert_Knowledge, Scenario)
Model_r = Build_Risk_Assessment_Model(*r*)
Step 3: Perform Risk evaluation by Monte Carlo simulation
Input: Decision, Risk Assessment Model (Model_r), Data Quality Features
Output: Simulated Risk Averages for Each Decision
Initialize Risk_Results = []
Construct distribution and variance for data with quality issues (Decision, Data_Quality_Features)
while simulation results have not converged **do**
    Generate random data samples (Sample_Data) within the uncertainty range
    Perform risk assessment:
        Risk = Model_r(Sample_Data, decision)
    Add Risk to Risk_Results
end while
Calculate the simulated risk average for this decision:
    Risk_Average = Calculate_Average(Risk_Results)
Associate Risk_Average with this decision

3.2.2. Decisions to Restore the Microgrid to Operational Condition

In microgrid maintenance logistic operations, key decisions include scheduling routine inspections, detecting anomalies during inspections, determining maintenance intervention optimal dates, deciding on repair actions, prioritizing maintenance tasks, planning emergency repairs, allocating maintenance personnel, managing the inventory of spare parts, etc.

3.2.3. Proactive Control and Predictive Maintenance Decisions

High degrees of foresight and responsiveness are key characteristics of a microgrid's resilience decision process involving active control and predictive maintenance compared with conventional control and maintenance. Active control and predictive maintenance use real-time monitoring, data analysis, and predictive maintenance task-scheduling algorithms, which can rely on data analysis and machine learning to pre-identify potential failures and perform predictive maintenance. Following crisis scenarios related to disaster situations, microgrids trigger these functionalities to respond and recover quickly. Sensor networks are used to monitor equipment parameters such as temperature, current, voltage, and vibration to decide in real time that maintenance operations are arranged on time. Maintenance personnel and spare parts can thus be quickly deployed to mitigate the disaster effects through logistic decisions and maintenance strategies of crisis conditions. This approach enhances the flexibility and recovery speed of microgrid resilience control, ensuring its stable operation under the worst conditions.

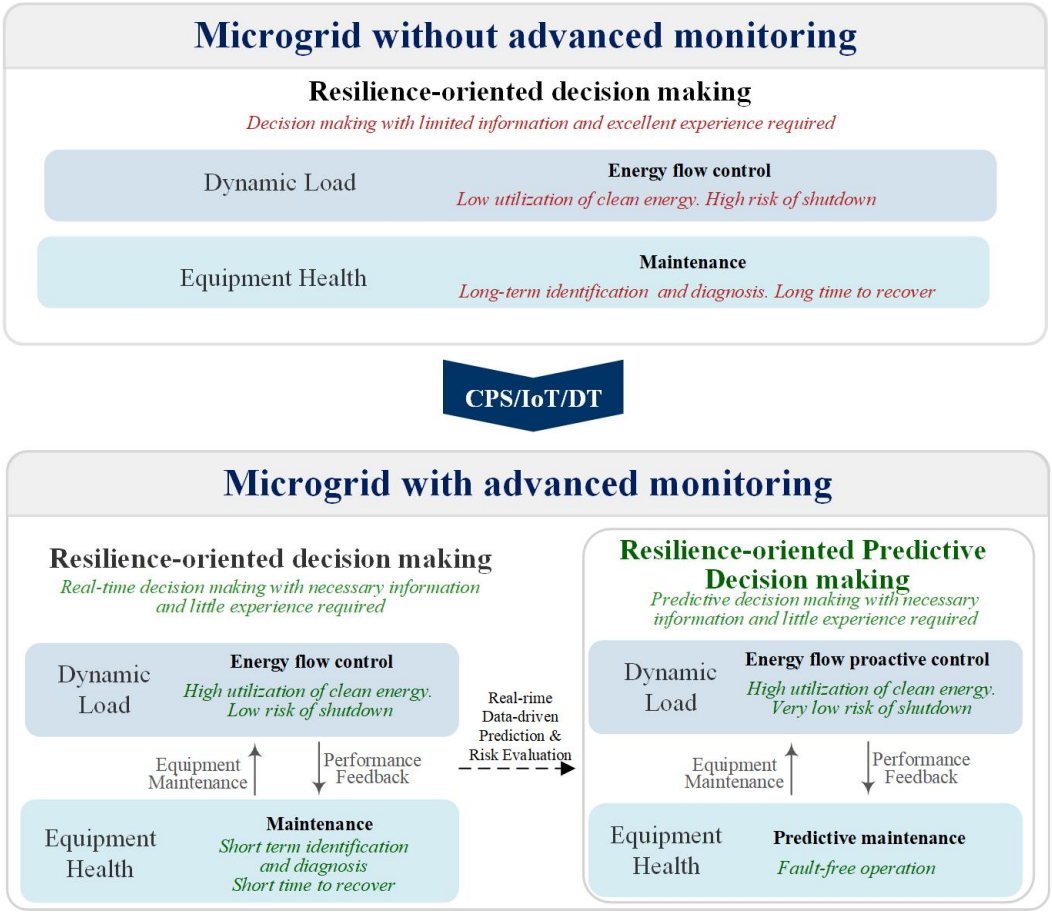

Figure 5. Resilience-oriented decision making in microgrid.

3.3. Decision-Making Risk Identification

According to [27,28], decision making can be classified as structured, semi-structured, or unstructured, which can make the corresponding risk difficult to identify and assess. The difficulty lies in the fact that the risk occurrence date, propagation, and impact are difficult to determine, model, and thus quantify [29]. Although there is no consensus on the definition of risk in academia, scholars in different fields have their own understanding of it, as shown in Table 1.

In engineering, some scholars regard risk as the possibility of a disaster event [30], such as a plane or train crash, an explosion of a chemical reactor, a mine gallery collapse, etc. Such disasters often occur very quickly, with unacceptable consequences or losses difficult to assess. Therefore, most research focuses on investigating methods to avoid the occurrence of such events.

Some scholars consider risk the loss caused by disaster events to human society [31,32], which are evaluated by the measurement of the scope of areas flooded by floods, the scope of a river's pollution by industrial waste, etc. The occurrence frequency of such disaster events is relatively low and has a certain degree of predictability. Therefore, this research study focuses on taking actions to avoid or mitigate the disaster event's impact on potential victims.

In this paper, we define decision risk as the potential loss caused by potentially damaging events when making a decision. To evaluate the risks faced when making decisions, the damaging events likely to occur in the decision-making scenario and the detrimental losses deserve to be studied.

The risks involved in decision making fall into one of the three aforementioned categories and may lead to one of the following four consequence types: safety loss, equipment loss, energy (cost increase), and customer complaints.

Table 1. Research focus on risk categories.

Risk Definition	Examples	Rate of Evolution	Consequences	Research Focus
Possibility of accident	Airplane crash	Rapid	Unacceptable/hard to assess	Prevention of catastrophic events
Losses from events	Impact of flood basins and chemical pollution effects	Gradual	Predictable/changeable	Mitigating the impact of disasters on potential victims

3.3.1. Risks in Real-Time Energy Flow Control Decisions

In real-time energy flow control decisions, wrong decisions may result in undesirable events in multiple aspects and lead to serious damage. Table 2 details a list of possible detrimental events in each aspect, the occurrence probability of related events, and the possible consequences.

Table 2. Risks in real-time energy flow control decisions.

Aspect	Hazardous Events	Probability of Events	Loss
Safety hazards	Electrical fire	Low–medium	Facility damage, personal injury, legal liability, and compensation costs
	Equipment short circuit	Medium	Electric shock, equipment damage, and emergency repair costs
Equipment damage	Equipment overload and damage	Medium–high	Increased equipment repair and replacement costs and shortened equipment lifespan
	Battery overcharging or deep discharging	Medium–high	Battery damage, shortened lifespan, thermal runaway risk, and fire
Power generation losses	Overuse of fossil fuels	High	Increased generation losses and higher operational expenses
	Frequent equipment failures	Medium–high	Increased maintenance and replacement costs and reduced generation efficiency due to downtime
Customer claims	Unstable power supply	Medium	Increased customer complaints and claims and damaged corporate reputation
	Power outage for critical loads	Low–medium	Data loss, business interruption, and compensation required for customer losses

3.3.2. Risks Considered in Decisions to Restore the Microgrid to Operational Condition

In the decision-making process of equipment maintenance, wrong decisions may raise various risks. Table 3 details the list of possible damaging events, their occurrence probability, and possible damages. For example, insufficient maintenance frequency may result in excessive wear and failure of equipment, inaccurate failure prediction may cause serious damage to equipment, wrong maintenance actions undermine the safe operation of equipment, and power outages may trigger customers' complaints.

Table 3. Risks in decisions to restore the microgrid to operational condition.

Aspect	Undesirable Events	Probability of Undesirable Events	Loss
Safety hazards	Equipment-related safety incidents	Low–medium	Fires, explosions, and facility damage
	Injuries during maintenance	Medium	Increased legal liability and compensation costs
Equipment damage	Insufficient maintenance frequency	Medium–high	Increased wear and tear, and higher repair and replacement costs
	Inaccurate fault prediction	Medium–high	Failure to detect faults timely, leading to severe equipment damage
Power generation losses	Over-maintenance	Medium	Higher maintenance costs and downtime, reduced generation efficiency
	Energy waste	Medium	Reduced equipment efficiency, and higher energy consumption and generation losses
Customer claims	Power outages	Medium–high	Increased customer complaints and claims, and compensation for business interruption
	Reduced service quality	Medium	Lower customer satisfaction and higher customer churn risk

3.3.3. Risks Considered in the Resilience Process Based on Proactive Control and Predictive Maintenance Decisions

In a resilience process based on proactive control and predictive maintenance decisions, several risks must be considered for safe and efficient operation of the microgrid. Risks include safety hazards, equipment damage, power generation losses, and customer claims. Table 4 below details potential hazardous events, their likelihood, and associated losses. For example, insufficient real-time monitoring can result in undetected equipment degradation or failure, an algorithm's incorrect prediction can result in unexpected failures, and improper demand response may cause instability in the power supply.

Table 4. Risks in proactive control and predictive maintenance decisions.

Aspect	Undesirable Events	Probability of Undesirable Events	Loss
Safety hazards	Faulty equipment predictions	Low–medium	Fires, explosions, and facility damage
	Injuries during maintenance	Medium	Maintenance personnel injuries, and increased legal liability and compensation costs
Equipment damage	Insufficient real-time monitoring	Medium–high	Undetected equipment degradation, and increased repair and replacement costs
	Incorrect predictive algorithms	Medium	Unexpected equipment failures and severe equipment damage
Power generation losses	Inefficient energy dispatch	Medium–high	Higher operational costs and increased energy consumption
	Delayed maintenance actions	Medium	Increased downtime, and higher maintenance and replacement costs
Customer claims	Unstable power supply	Medium	Increased customer complaints and claims, and compensation for service disruptions
	Inadequate power for critical loads	Low–medium	Data loss, business interruption, and compensation for customer losses

4. Applications and Practice

To evaluate our decision risk prediction approach through numerical experiments, we applied it to a model of a real microgrid fed by PV power, assigned to supply power to an

industrial textile production plant in Ghana, West Africa. We designed instrumentation based on a sensor network to collect data on the microgrid, as described in the paragraphs below, and collected data over 14 months.

4.1. Solar Plant Microgrid

4.1.1. Microgrid Description

As Figure 6 depicts, the microgrid consists of several components: power sources, inverters, switching devices, a communication device, a power cabinet, a monitoring system, and a connection to the auxiliary power grid in crises. The details of each element and their relations are provided below:

- The solar panels represent energy sources, called modules. There are 5 sets of modules, each connected to an inverter.
- Inverters convert direct current (DC) from solar modules into alternating current (AC). The DC lines stemming from solar modules are drawn in blue, while the AC lines are red.
- The smart communication box serves as a hub that collects and analyzes data from the inverters. It bridges the inverters and communication lines (gray lines), which allows for the monitoring and control of the solar panels and inverters.
- The AC cabinet interconnects the inverters' output AC power and the auxiliary grid.
- The Point of Interconnection (POI) is an essential billing device that measures and monitors the power flow between the microgrid and the auxiliary grid. It is also connected to the smart communication box.
- The grid stands for the auxiliary power grid.
- The cloud allows for remote access to all data collected through the smart communication box for the whole system's performance management.
- The red and blue lines represent AC and DC power flows, respectively, while the gray lines signify communication links that allow for the integration and smart management of the system components and performance.

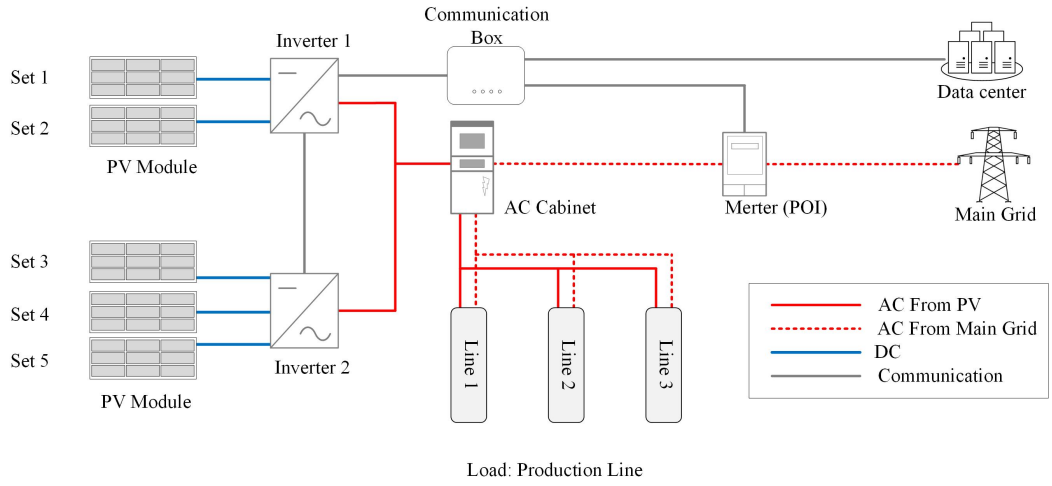

Figure 6. The architecture of an actual microgrid.

As exhibited in Figure 7, we supplemented the microgrid with a wireless sensor network, to enhance its monitoring capabilities. This information network offers redundant additional independent channels to collect and transmit data in the event of severe damage to wired links under critical conditions. The resulting information network system includes various components linked through both power and communication lines, as well as wireless channels, emphasizing efficient energy management and the real-time health monitoring of the microgrid components. Below, we detail how the sensor network performs within the system.

A wireless/PLC sensor transceiver is embedded in each module, inverter, POI meter, AC cabinet, and smart communication box in the microgrid to monitor various parameters, such as voltage, current, frequency, ambient, component temperatures, humidity, component state, performance, etc. The wireless/PLC device network improves the responsiveness and adaptability of this new microgrid system and enables its advanced monitoring, safe operation, and the control of its resilience.

The networked monitoring system ensures that any issue detected in a component, in the power flow quality and stability, or in the external auxiliary grid unstable power supply is quickly identified and handled. It also ensures robust, real-time communication between the hardware components and the cloud and that data are not only collected but also reliably transmitted to the cloud monitoring systems, which enables seamless data integration across the microgrid and its monitoring network. The latter not only enables for the monitoring and detecting in real time of all weaknesses emerging due to degradation within the microgrid infrastructures but also significantly reduces risks in resilience control decision-making processes.

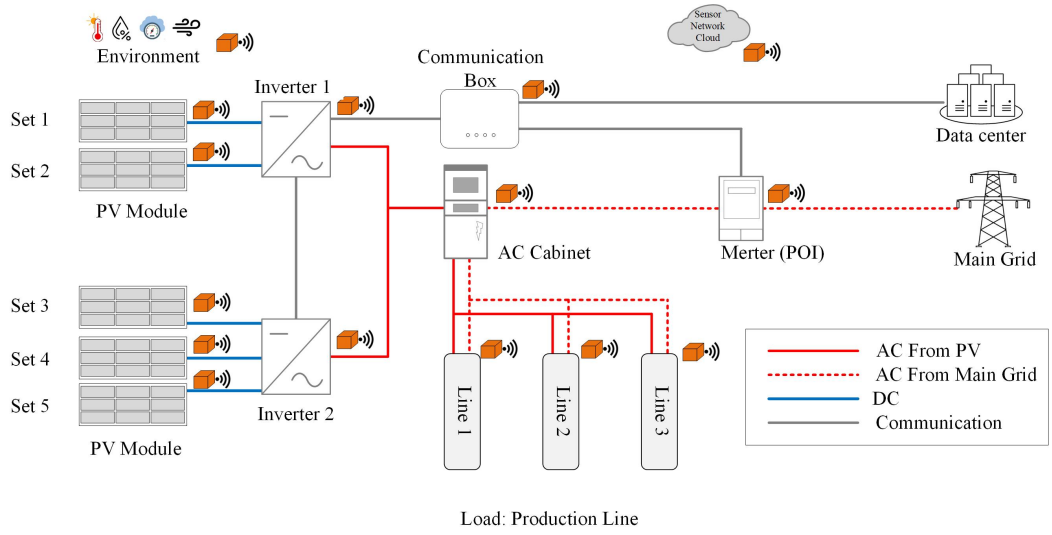

Figure 7. The architecture of an actual microgrid with sensor network.

4.1.2. Microgrid Sample Data

Data collected from the microgrid are used to make various decisions and assess various risks to provide the power needed by the production plant on demand. Figure 8 depicts power production from the photovoltaic (PV) panels under various sunlight conditions, through data sample curves of the DC power generated by solar panels and the related channels of Maximum Power Point Tracking (MPPT). The curves detail the output power produced by the microgrid PV panels over one month (May 2022). The first graph displays the daily direct-current (DC) power output from the inverter, while the second graph offers insights into the performance of MPPT channels, which are crucial to optimizing energy harvesting from PV panels. These data not only help to understand the daily variability in solar power generation but also aid in pinpointing potential issues in the solar array, such as malfunctions or degradation within specific MPPT channels.

Figure 9 displays, with distinct color lines, the current output of an inverter over a day, from five MPPT channels. These curves illustrate the dynamic interaction between solar irradiance and an inverter's whole-day performance. In the graph, the x-axis represents the daytime, spanning from 12:00 a.m. to 11:59 p.m., while the y-axis is the current in ampere (A).

As expected, the power output of MPPT channels increases from near-zero current at sunrise at around 6:00 a.m., with solar irradiance, to the peak at noon; then, it declines post-noon toward near-zero current by 6:00 p.m. and remains at zero current all overnight.

This typical profile of photovoltaic energy production explains the need to ensure a backup energy source during periods of decline or insufficiency for various reasons, including the failures of irradiation, PV panels, and components performance degradation in the electrical microgrid, in addition to critical adverse climatic conditions.

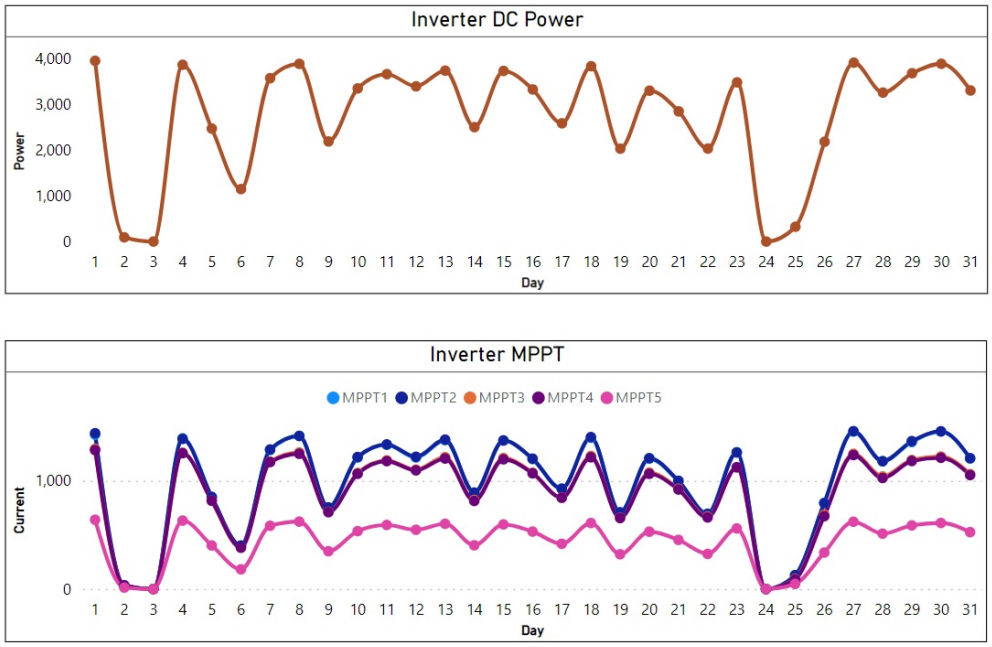

Figure 8. Example of solar panel inverter DC power and five related MPPT daily measurements.

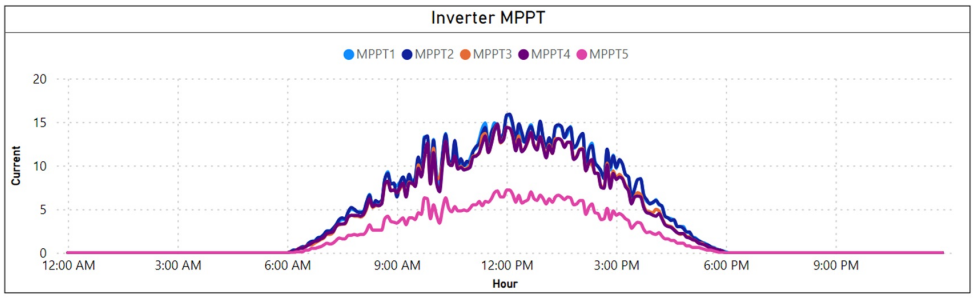

Figure 9. Example of hourly MPPT measurements of the output current of five PV panels inverters.

Based on historical data, one can predict the expected PV power generation and its variance over the following hours, depending on the current weather conditions and local time. The five $MPPT_i, (i = 1, \ldots, 5)$ are synchronized to satisfy power demand, but although they are probably all similar and operate under similar conditions, one observes a weaker $MPPT_5$ inverter power output. Thus, the under-performance of $MPPT_5$ affects the overall microgrid energy output predictions. This observation suggests a potential issue, including less sunlight received by the corresponding PV due to improper installation, non-performant PV panel, failing PV panel, failing inverter, partial shading, sub-optimal panel orientation, or lack of maintenance.

4.1.3. Decision Support Hypothesis Based on Microgrid Historical Data

The data collected hourly will serve to make various decisions:

- Fault detection by using estimated discrepancies between the predicted and actual outputs to identify potential issues previously mentioned.
- Microgrid energy production, real-time power flow control, power distribution, energy storage, and power procurement from the auxiliary grid.

- Predictive maintenance: The real-time monitoring of the MPPTs' outputs, with the microgrid system networked components' health prognosis and predictive maintenance scheduling for resilient optimal operation.

4.2. Decision Process 1: Power Source Options in Microgrid Energy Management

4.2.1. Decision-Making Model

Safe, optimal, and resilient microgrid operation requires continued balance and stability control of energy flow between sources and loads of the textile production lines while maximizing the use of renewable energy sources, even under critical operating conditions. By rationally adjusting the load, the factory in the microgrid not only maximizes its use of renewable energy but also enhances the overall resilience of the system. Load management is a critical component of the microgrid, as it enables the factory to dynamically respond to fluctuations in power supply, especially during periods of instability or unexpected changes. This flexibility in load management helps maintain the balance between power generation and consumption, thereby reducing the risk of overloading the system and ensuring a more reliable and sustainable operational model.

In this case, the textile factory operates three production lines, each with a power load of 130 kW and a minimum power supply requirement of 110 kW, as illustrated in Figure 10. Each production line can be powered by either solar energy or the auxiliary grid, or it can remain shut down. This power source configuration could be extended with additional renewable energy sources, but the problem will remain identical, so we limit this paper to the PV panels' power source.

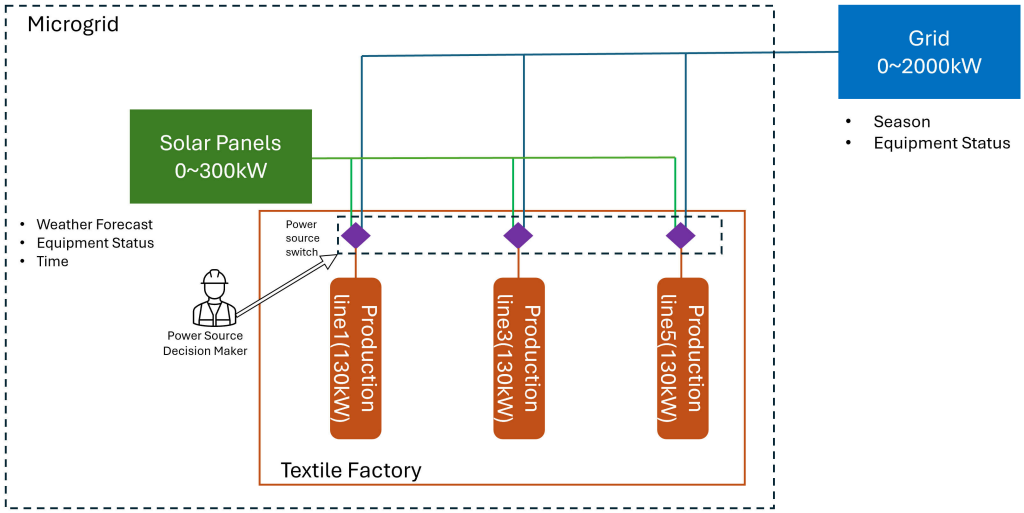

Figure 10. Control options of microgrid power sources.

The decision-making process involves using the predicted solar power generation to adjust the power production to each manufacturing line during employee breaks (every two hours) and switching between auxiliary grid power and solar power. The goals of the decision include minimizing power costs and minimizing unexpected downtime risk; the objective functions are shown as functions (1) and (2).

$$\text{Minimize } Cost = \text{ Minimize } \sum_{i=1}^{3}\left(P_{i,t}^{g} \cdot C^{g} + P_{i,t}^{pv} \cdot C^{pv}\right), \tag{1}$$

$$\text{Minimize } Risk = \text{ Minimize } \sum_{i=1}^{3}\left(200 \times S_i \times \pi_i^F + 100 \times \pi_i^F \times \Delta t_i^F\right), \tag{2}$$

where the following apply:

C^{pv}: cost of PV power—0.051 USD/kWh;

C^g: cost of auxiliary grid power—0.177 USD/kWh;
$P_{i,t}^{pv}$: PV power supply to the i^{th} manufacturing line at time$t$ (kW);
$P_{i,t}^{g}$: auxiliary grid power supply to the i^{th} manufacturing line at time t (kW);
i : index for each manufacturing line $(i = 1, 2, 3)$;
t : time index of decision making;
π_i^F: probability of failure of the i^{th} manufacturing line;
S_i : indicator function for whether the i^{th} manufacturing line is for a critical product (equal to 1 if it is a critical product and 0 if it is not a critical product);
Δt_i^F: duration of downtime of the i^{th} manufacturing line.

Objective function (2) indicates that for certain products, the production line cannot be stopped within two hours of processing. The current work in progress is scrapped if the line halts within this period, incurring an additional loss of USD 2000 per stop. For other products, a stop in the production line results in a waste of USD 1000 per stop.

The objective functions are supplemented with four additional constraints to consider the energy management requirements within the microgrid system.

$$P_{i,t}^{g} + P_{i,t}^{pv} \leq L_i^{\text{normal}}, \quad \forall i, t, \tag{3}$$

$$P_{i,t}^{g} + P_{i,t}^{pv} \geq L_i^{\min}, \quad \forall i, t, \tag{4}$$

$$\sum_{i=1}^{6} P_{i,t}^{pv} \leq S_t, \quad \forall t, \tag{5}$$

$$eg(P_{i,t}^{pv} > 0 \wedge P_{i,t}^{blue} g > 0), \tag{6}$$

$$\pi_i^F(P_{i,t}) = \begin{cases} 0 & \text{if } P_{i,t} \geq 120 \text{ kW} \\ 0.1 & \text{if } 110 \leq P_{i,t} < 120 \text{ kW} \\ 1 & \text{if } P_{i,t} < 110 \text{ kW} \end{cases}, \tag{7}$$

where the following apply:
L_i^{normal} is the normal operating load for the i^{th} manufacturing line (130 kW).
$L_i^{\min}$ is the minimum operating load for the i^{th} manufacturing line (110 kW).
S_t is the total solar power available at time t (kW).
$P_{i,t}$ is the power supply to the i^{th} manufacturing line at time t (kW), and $P_{i,t} = P_{i,t}^{g} + P_{i,t}^{pv}$.

Equations (3) and (4) specify that each manufacturing line must consume power ranging from 110 kW to 130 kW. Equation (5) requires that the total PV power distributed to all manufacturing lines does not exceed the overall PV power generated. Equation (6) requires that each manufacturing line is powered by a single source to ensure optimized energy management. Consequently, PV power generation $P_{i,t}^{pv}$ and auxiliary power supply $P_{i,t}^{g}$ do not simultaneously provide non-zero power. Equation (7) explains that the shutdown probability is 10% when the power supply of the manufacturing line lies between 110 and 120 kW and is 100% when the power supply is lower than 110 kW.

Genetic algorithms (GAs) are extensively utilized to address multi-objective optimization problems successfully, yielding a Pareto frontier solution set, which represents the optimal trade-off. In this paper, Monte Carlo (MC) simulation-based Algorithm 2 elucidates the risk assessment procedure for shutting down a manufacturing line.

Furthermore, the detailed implementation of the genetic algorithm is meticulously delineated in Algorithm 3. To accelerate algorithm computation convergence, a Monte Carlo risk simulation result caching mechanism is applied for each scenario, preventing redundant calculations. Given that the results of the Monte Carlo risk simulation assessment for the same solution may vary slightly, we incorporated the concept of risk tolerance. By

employing a non-dominated sorting function, this approach not only maximizes the inclusion of diverse risks but also ensures that the solution set encompasses as many potential solutions as possible.

Algorithm 2 : Risk assessment of production line downtime with MC simulation

Input: *power_grid*, *power_solar*, *grid_reliability*(), *line_shutdown*(), *risk*()
Output: risk (potential loss when this production line shutdown)
if *power_grid* > 0 **then**
  Reliability = *grid_reliability*(2, temperature, rainfall)
  $P_{\text{stop}} = 1 -$ Reliability
end if
if *power_solar* > 0 **then**
  for $i = 1$ **to** N **do**
    $simulated\_power\_solar = \text{sample}(power\_solar, \text{std})$
    $simulated\_P\_stop = \text{line\_shutdown}(simulated\_power\_solar)$
  end for
  $P_{\text{stop}} = \text{average}(simulated\_P\_stop)$
end if
$risk = risk(P_{\text{stop}})$, as shown in Equation (2)
Return risk

4.2.2. Uncertain Information

Uncertainty in Solar Power Generation

In the prediction process of PV power generation, the completeness of equipment health information is crucial for prediction accuracy. When a comprehensive understanding of the PV power system's health status is available, the predictions tend to be more precise. However, a lack of critical device information, for instance, the unknown health status of the inverter, may imply that the inverter is faulty, thereby affecting the normal operation of the entire PV power system. Similarly, if the health status of the PV panel unit is undetermined, the unit is likely in a failure state.

The actual PV power output P_t^* can be modeled as a random variable:

$$P_t^* = \mu_t^P + \sigma_t \cdot \epsilon_t, \tag{8}$$

where the following apply:

ϵ_t is a random variable representing the uncertainty at time t; $\epsilon_t \sim \mathcal{N}(0, 1)$, assuming ϵ_t is drawn from a normal distribution with mean 0 and variance 1;
μ_t^P is the expected PV power output value at time t (kW) and is influenced by factors such as the daytime, the expected cloud cover, and the historical PV power output values;
σ_t is the standard deviation of the PV power output at time t (kW).

Prediction of PV Power Output Values in Two Hours and Uncertainty Under Normal Conditions

Example of data under normal operating conditions:

- For the time period 6 a.m. to 7 a.m.: μ_t = 150 kW and σ_t = 20 kW;
- For the time period 7 a.m. to 8 a.m.: μ_t = 170 kW and σ_t = 25 kW.

Under normal operating conditions, one can predict the actual PV power output by using the given distribution. The uncertainty σ_t accounts for variability in sunlight, panel efficiency, and other minor factors.

Impact of component failure on solar power generation

When a specific component (e.g., a DC line or inverter) fails or its state is degraded, the prediction model needs to adjust both the expected output μ_t and the uncertainty σ_t to reflect this degradation.

Algorithm 3 Multi-objective genetic algorithm for pareto front determination

Input:
$N = 1000$—Number of solutions in the population,
$G_{max} = 1000$—Maximum number of generations,
$p_c = 0.8$—Crossover probability,
$p_m = 0.1$—Mutation probability,
$risk\_tolerance = 1.05$—Tolerance threshold for risk
Output: Pareto front containing non-dominated solutions
Initialize P_0 with random solutions
Initialize an empty dictionary *RiskCache* to store risk values for each unique solution
for each individual in P_0 **do**
  if solution in *RiskCache* **then**
    Retrieve the risk value from *RiskCache*
  else
    Compute the risk using Monte Carlo simulation
    Store the computed risk in *RiskCache*
  end if
end for
for $g = 1$ to G_{max} **do**
  Select parents from P_{g-1} based on fitness (cost and risk)
  Perform crossover on selected parents to create new offspring O_g
  for each pair of parents **do**
    if rand() $< p_c$ **then**
      Apply crossover operation to create two offspring
    else
      Copy parents to O_g unchanged
    end if
  end for
  Apply mutation to O_g
  for each offspring **do**
    if rand() $< p_m$ **then**
      Mutate random parts of the offspring
    end if
  end for
  for each individual in O_g **do**
    if solution in *RiskCache* **then**
      Retrieve the risk value from *RiskCache*
    else
      Compute the risk using Monte Carlo simulation
      Store the computed risk in *RiskCache*
    end if
    Apply risk tolerance: if $risk \leq risk\_tolerance$, adjust fitness to improve dominance level (e.g., reduce the cost objective)
  end for
  Combine O_g with P_{g-1} to form R_g
  Apply non-dominated sorting to R_g to identify levels of dominance
  Update P_g with the best solutions found (keeping the population size constant)
  if a termination condition is met **then**
    break
  end if
end for
Collect all non-dominated solutions from P_g
Return these solutions as the Pareto front

- Expected output μ_t adjustment: If a key component, such as an MPPT unit, fails, the expected output μ_t should be reduced according to the performance degradation

observed. For example, if MPPT5 shows 30% lower output than the other MPPTs due to partial failure, the overall μ_t for the system might be reduced by a corresponding percentage. Thus, the following apply:
From 6 a.m. to 7 a.m., the adjusted $\mu_t = 150x(1 - 0.3) = 105$ kW.
From 7 a.m. to 8 a.m., the adjusted $\mu_t = 170x(1 - 0.3) = 119$ kW.

- Uncertainty σ_t adjustment: When equipment is degraded or missing, the uncertainty in PV power generation increases due to the added variability and reduced reliability. For example, with the failure of MPPT5, σ_t might increase to reflect the additional unpredictability.
From 6 a.m. to 7 a.m., the adjusted $\sigma_t = 20 + 10 = 30$ kW.
From 7 a.m. to 8 a.m., the adjusted $\sigma_t = 25 + 10 = 35$ kW.

Health Status Information

When the health status information of the equipment indicates failure or degradation, the prediction model becomes

$$\check{P}_t^* = \check{\mu}_t^P + \check{\sigma}_t \cdot \epsilon_t, \tag{9}$$

where the following apply:
$\check{\mu}_t^P$ reflects the decreased expected output due to equipment failure;
$\check{\sigma}_t$ reflects the decreased uncertainty due to the equipment failure.
For example, if ϵ_t is sampled as 0.5 for the first hour and -0.3 for the second hour the following apply:
From 6 a.m. to 7 a.m.: $S_t = 105 + 30 \times 0.5 = 120$ kW.,
From 7 a.m. to 8 a.m.: $S_t = 119 + 35 \times (-0.3) = 108.5$ kW.

Uncertainty in Auxiliary Grid Reliability

Based on the company's historical monitoring data, we analyzed microgrid reliability performance under different climatic operating conditions. During the dry season, when temperatures exceed 33 °C, the overall load on the regional grid increases significantly, leading to fault occurrence on average every two days. Based on this, we calculated that the microgrid reliability for the next two hours is 95.92%. On the other hand, during the rainy season, if the rainfall intensity exceeds 2 mm per hour (i.e., it reaches the level of a storm), the microgrid failure frequency/rate increases to once a day. Based on these data, we predict the microgrid reliability to drop to 92.04% over the next two hours. For other climatic conditions, the stability of the grid significantly improves, with fault occurrence on average only once every three weeks. Therefore, during these periods, the microgrid reliability for the next two hours is as high as 99.60%.

$$R_{\text{grid}}(t, T, R) = \begin{cases} e^{-0.02087t} & \text{if } T > 33 \\ e^{-0.04185t} & \text{if } R > 2 \\ e^{-0.002t} & \text{otherwise} \end{cases}, \tag{10}$$

4.2.3. Example of Decision Making at Time t

On a specific day, from 10 a.m. to 12 p.m., the anticipated PV power output for the subsequent two-hour period is 240 kW, with an uncertainty of 35 kW as calculated by using Equations (8) and (9). Additionally, the ambient temperature is recorded as $T = 29°$C and rain as $R = 3$ mm/h.

In light of these data, the decision-making pathways outlined in Algorithms 2 and 3 guide the determination of the Pareto Front, as illustrated in Table 5. The first two solutions show the lowest electricity cost, while the last two show the lowest risk. Due to the Monte Carlo simulation calculation, their risk values are not completely consistent. This meticulous process ensures that the energy management system can opt for solutions that best balance the competing objectives, thereby optimizing the overall performance.

Table 5. The Pareto Front determination.

Line 1	Line 2	Line 3	Cost (USD)	Risk (USD)
(0, 110) [1]	(0, 110)	(130, 0)	68.46	233.71
(130, 0) [2]	(0, 110)	(0, 110)	68.46	232.35
(130, 0)	(0, 120)	(0, 120)	70.5	223.81
(0, 120)	(0, 120)	(130, 0)	70.5	225.36

[1] Production line 1 is powered by PV power with a power supply of 110 kW. [2] Production line 1 is powered by the auxiliary power grid with a power supply of 130 kW.

In this case, if the uncertainty in solar power generation is disregarded and only the lowest-cost option is chosen for energy management, the potential risk may reach its maximum. Without the construction of a reliability model for the local environment and the power grid using the IoT, it would be impossible to effectively predict the overall reliability of the grid. Similarly, without monitoring the operational status of power generation equipment in the microgrid, the uncertainty in generation capacity cannot be accurately assessed. Furthermore, without the IoT-based monitoring of solar energy resources in the plant's environment, it would not be feasible to combine meteorological data to accurately predict solar power generation efficiency at any given time. In the absence of these predictive capabilities, relying solely on experience-based judgments for decision making, simulation analysis shows that the potential risk could reach its maximum.

4.3. Decision Process 2: Scheduling Maintenance Actions in Microgrid

4.3.1. Decision-Making Model

In this case study, the decision aims to schedule predictive maintenance actions while minimizing the time to perform all maintenance tasks on a finite horizon H, starting from the occurrence of a disastrous event. Figure 11 highlights the actions of maintenance teams on a microgrid which is identical to that in Figure 10. The predictive maintenance actions are scheduled according to an order defined by the microgrid components' operation safety level, importance in the system architecture, and then failure probability. The components responsible for the safety of the human operators involved in maintenance actions and with the highest failure probability are fixed first, followed by important components critical for the microgrid's main function with the highest failure probability, and finally, the remaining components are treated in descending order of failure probability. The total time spent to fix a faulty component is the sum of the time to identify the failure and the time to repair it.

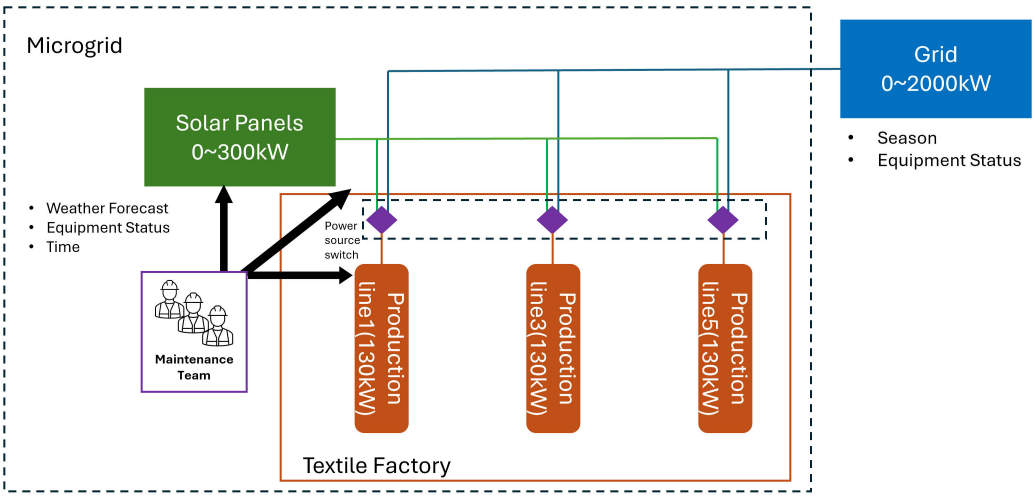

Figure 11. Microgrid resilience control decision making based on a maintenance process.

The objective function for maintenance action scheduling or decision [33] is shown in Function (11).

$$\text{Minimize } T_{\text{total}}(H) = \sum_{i=1}^{N} \sum_{m \in H} [(\tau_{m,i} + t_{m,i}) - r_{m,i} + \max(0, (\tau_{m,i} + t_{m,i}) - d_{m,i})], \quad (11)$$

where the following apply:

$T_{\text{total}}(H)$ is the total maintenance time to be minimized over the horizon H;
$\tau_{m,i}$ is the time required to identify the m^{th} fault in the i^{th} component of the microgrid;
$t_{m,i}$ is the time required to repair the m^{th} fault in the i^{th} component of the microgrid;
$r_{m,i}$ is the planned repair time for component m on manufacturing line or PV panels i;
$d_{m,i}$ is the due time to repair the m^{th} fault in the i^{th} component of the microgrid;
$(\tau_{m,i} + t_{m,i}) - r_{m,i}$ represents the difference between actual total time (identification + required time) and planned repair time $r_{m,i}$. If the actual time exceeds $r_{m,i}$, this difference contributes positively to the total cost to be minimized;
$\max(0, (\tau_{m,i} + t_{m,i}) - d_{m,i})$ introduces a penalty if the actual total time (identification + repair) $(\tau_{m,i} + t_{m,i})$ exceeds the deadline $d_{m,i}$. The penalty is equal to the amount by which the deadline is exceeded. If the actual total time is less than or equal to the deadline, this part is zero;
$\tau_{m,i} \sim U(a_{m,i}, b_{m,i})$ is the uniform law, with $a_{m,i}$ being the minimum possible time to identify the fault and $b_{m,i}$ being the maximum possible time to identify the fault.

In the current application, starting from the disruptive event time as the initial instant, the resilience time horizon is given by

$$\sum_{i=1}^{N} [(\tau_{1,i} + t_{1,i}) - r_{1,i}], \quad (12)$$

Then, the values of $m \geq 2$ apply to predictive maintenance action scheduling following the resilience time horizon.

The objective function is supplemented with three additional constraints to consider.

$$\sum_{m \in H} x_{m,i} \leq \text{Maintenance Capacity}, \quad (13)$$

$$\text{If } \lambda_{m,i} > \lambda_{n,i}, \text{ then } t_{m,i} \leq t_{n,i}, \quad (14)$$

$$\tau_{m,i} + t_{m,i} \leq d_{m,i}, \quad \forall m \in H, \quad (15)$$

Function (13) is a maintenance resource constraint. The maintenance team may have a limited number of resources (technicians, spare parts, etc.), which limits the number of components m that can be repaired simultaneously.

Function (14) is a priority based on failure rate. The first to be repaired should be components with a higher failure rate $\lambda_{m,i}$ for safety reasons and then critical components according to their reliability importance [34], more specifically pathway-type *p-FV* reliability importance [35].

Function (15) is a deadline compliance constraint. Repairs should ideally be completed before the deadlines $d_{m,i}$ to avoid excessive penalties. So, the objective function seeks to minimize the overall time required to identify and remedy flaws in the microgrid system. It takes into account planned repair periods, time limits, and the complexity of maintenance tasks, with the goal of minimizing delays and time overruns. The accompanying constraints ensure that repairs are completed efficiently and prioritized based on available resources and operating requirements.

Decision model contribution to microgrid resilience. This decision-making model enhances microgrid resilience by ensuring that maintenance tasks are carried out efficiently,

resources are optimally used, and system downtime is minimized, all of which are crucial to maintaining the availability and stability of the microgrid. These improvements in maintenance management contribute to a more robust, safe, and adaptable microgrid infrastructure capable of withstanding and quickly recovering from disruptions.

Adjallah et al. [33] present a robust algorithm that leverages the Flow-Time and Tardiness Response (FTR) function combined with an urgency criterion to effectively prioritize tasks across multiple machines. The FTR function helps minimize total maintenance costs while meeting availability requirements, and the inclusion of the urgency criterion ensures that critical tasks are prioritized. Our model builds upon this foundation, applying these principles to the context of renewable energy microgrids, which differ from traditional manufacturing systems due to their integration of intermittent energy sources and heterogeneous components (solar panels, inverters, etc.). While the authors in [33] demonstrate excellent performance in minimizing maintenance costs in distributed industrial systems, our approach extends this to address the socio-technical aspect and environmental complexities inherent to microgrids. Specifically, our model focuses not only on cost minimization but also on enhancing resilience by scheduling predictive maintenance actions based on real-time data from sensor networks and optimizing system recovery after disruptions.

The model ensures that maintenance resources are used efficiently. By prioritizing tasks based on factors like the safety, failure rate, and criticality of components (indicated by their planned repair times and deadlines), the system can better allocate technical resources and spare parts. This prevents the overuse or underuse of resources, maintaining a balance that is crucial for steady microgrid operation.

By optimizing the components' fault identification and repair times, the model minimizes system downtime. The indicator is a critical parameter in microgrid resilience, as the prolonged inactivity of any component can lead to failures in providing continuous power. The decision model's ability to reduce the duration of repair and maintenance actions directly enhances the operational availability of the microgrid.

The model uses a probabilistic approach to predict faults and schedule maintenance. This predictive aspect is crucial to preempting failures before they occur, which is a significant component of resilience. Predictive maintenance allows the system to address potential failures proactively, thus avoiding unexpected breakdowns that could compromise the entire grid.

4.3.2. Decision-Making Risk Simulation Subject to Information Uncertainty

Based on the background described above, we constructed a simulation process by using Python, as shown in Algorithm 4. Multiple decisions are formulated based on the information about PV power generation. Based on existing decisions, uncertain information is processed and incorporated into the simulation to calculate the expected risk. For deterministic treatment methods, when certain information is missing, the current decision risk is assessed according to the worst-case scenario.

Simulation of real-time scheduling of predictive maintenance actions. Let us assume that the predictive maintenance policy has enabled the preparedness for maintenance intervention on components most likely to fail in case of critical events due to their weakness and remaining useful life. It then becomes easy to assign priorities to components in the post-disruption diagnosis process and schedule predictive maintenance actions accordingly while relying on the available real-time data and information. Here, the main objectives of this simulation are to assess the effectiveness of predictive maintenance action real-time scheduling in minimizing downtime and evaluate its effects on breakdowns and photovoltaic output power generation. The focus is on how to optimize the real-time scheduling of predictive maintenance actions to reduce the overall downtime and improve the microgrid's performance and quick recovery. As shown in Table 6 and Figure 6, 5 PV modules contribute equally to the microgrid power. Four different breakdown scenarios are investigated through simulation, with varying levels of performance drops (from 20% (0.8) to 100% (0)) after a sudden disruption, to benchmark the influence of both the traditional

and optimized real-time scheduling of maintenance actions. The aim is to demonstrate how the optimized real-time scheduling of maintenance can significantly reduce downtime and improve system resilience.

Table 6. System configuration and performance.

Sets of PV Module	Inverter	Power Drop (%)	Part of Output Power
Set 1	Inverter 1	20%	0.2
Set 2	Inverter 1	20%	0.2
Set 3	Inverter 2	20%	0.2
Set 4	Inverter 2	20%	0.2
Set 5	Inverter 2	20%	0.2

Algorithm 4 : Maintenance time optimization algorithm

Inputs:
N: Number of production line components or solar panels
H: Set of all components requiring maintenance
$T_{m,i}$: Randomly generated time to identify the fault for each component m on production line i, following a uniform distribution $U(a_{m,i}, b_{m,i})$
$t_{m,i}$: Estimated time to repair the fault for each component m on production line i
$r_{m,i}$: Planned repair time for each component
$d_{m,i}$: Deadline for each component
Output: Optimized identification and repair times for each component to minimize total maintenance time.
Initialization:
Initialize $T_{\text{total}}(H)$ to zero.
for each component m in H **do**
    Initialize $T_{m,i}$ and $t_{m,i}$.
end for
Fault Identification and Repair Simulation:
for each component m and each production line or solar panel i **do**
    Generate $T_{m,i}$ from the uniform distribution $U(a_{m,i}, b_{m,i})$.
    Estimate or set $t_{m,i}$ based on historical data or predictive maintenance algorithms.
end for
Calculate Total Maintenance Time:
for each component m in H **do**
    Compute the actual total time $T_{m,i} + t_{m,i}$.
    Calculate the time difference $T_{m,i} + t_{m,i} - r_{m,i}$ and add to $T_{\text{total}}(H)$.
    if $T_{m,i} + t_{m,i} > d_{m,i}$ **then**
        Add the penalty $(T_{m,i} + t_{m,i} - d_{m,i})$ to $T_{\text{total}}(H)$.
    end if
end for
Optimization Loop:
while not converged **do**
    Iteratively adjust $T_{m,i}$ and $t_{m,i}$ within their feasible ranges to minimize $T_{\text{total}}(H)$.
    Check constraints for each adjustment:
    Ensure $T_{m,i}$ remains within $[a_{m,i}, b_{m,i}]$.
    Calculate the new $T_{\text{total}}(H)$ and compare with the previous value to check for improvement.
end while
Result Presentation:
Output the optimized times and the minimized $T_{\text{total}}(H)$.

Maintenance and failure rate. For the simulation, components' reliability and maintenance data were extracted and adapted from IAEA Tecdoc-930 for generic components' reliability data [36], as shown in Figure 12 and Table 7. For all scenarios, the maintenance

team involves two technicians assigned to emergency maintenance actions and subsequent predictive maintenance activities. Table 8 summarizes maintenance performance in terms of maintenance repair time in the case of the standard maintenance procedure and optimized maintenance task scheduling for resilience control.

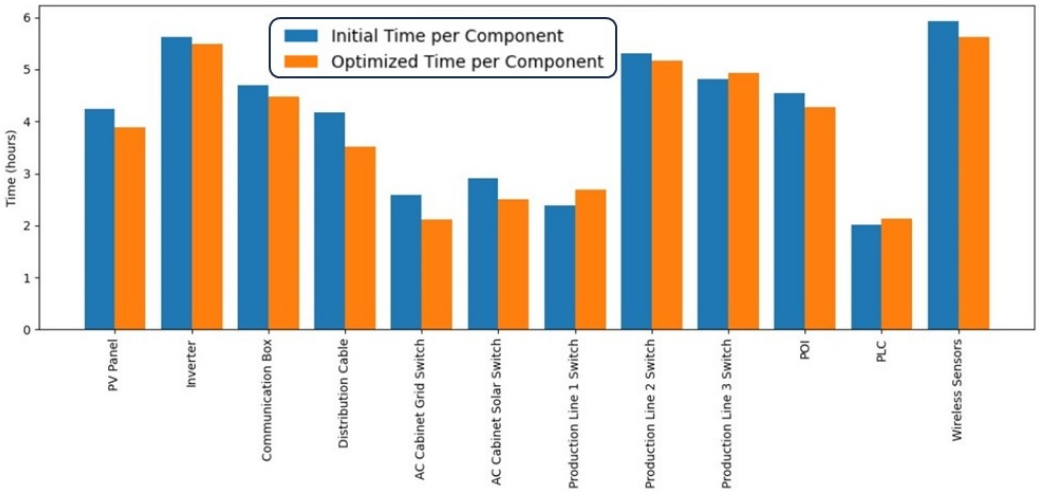

Figure 12. Components' maintenance time.

Table 7. Maintenance and failure rate data.

Component	Initial Time (h)	Optim. Time (h)	Failure Rate (10^{-6}/h)	Priority
Set of PV panels	4.25	3.88	114	3
Inverter	5.62	5.49	27	2
Switch	2.91	2.5	7	1

Table 8. Scenario of system failure after event.

Scenario	Set of Failed Elements	Drop in System Performance
1	1 PV panels set	20%
2	2 PV panels sets	40%
3	2 PV sets + 1 inverter	40%
4	2 PV sets + 1 inverter + 1 switch	100%

4.3.3. Result Analysis

Scenario 1. In this scenario, a single set of panels experiences a 20% performance drop due to a failure, and the standard and optimized maintenance action scheduling models were implemented. At time t_0, just after event, the system encounters a failure, resulting in a sudden performance drop from nominal performance P_0 to reduced performance P_1. This is indicated, in the PV power output curves in Figure 13, by the orange line, which spans from the breakdown to t_1, representing the time to identify the failure location. Maintenance actions are triggered at t_1, after the failure has been detected and identified. The optimized maintenance activities are completed at time t_2, and its effects on the microgrid total power output are displayed as a blue line, showcasing a quicker recovery process. This allows the system to return to full performance more rapidly. Additionally, the standard maintenance action scheduling effect is displayed as a red line. The latter takes a longer time to end at time t_3, as one can see. This delay prolongs the performance drop and delays the full recovery. The difference between t_2 and t_3 highlights the benefit of optimized maintenance, where performance is restored faster, minimizing the downtime. $\Delta_t = t_1 - t_0$ is the time required to identify the failure.

Scenario 2. In Scenario 2, the results show the system's performance undergoing a 40% drop, just after event, due to the breakdown of two panels sets. Similarly to Scenario 1, at

time t_0, the system drops from nominal performance P_0 to performance P_1, which is lower by 40%, as Figure 14 depicts. At time t_1, both the standard and optimized maintenance processes start to repair the broken components. Recovery begins, and performance improves over time. The blue line shows the end of optimized maintenance at t_2, where the system is fully restored to nominal performance (P_0). The red line indicates that standard maintenance takes longer and ends at t_3, showing slower recovery compared with the optimized process.

Figure 13. Scenario 1 simulation: 1 set of panels.

Scenario 3. In Scenario 3, the system experiences a 40% performance drop due to the failure of two panel sets and one inverter. In this scenario, according to safety and security requirements, the inverter must be fixed first before the PV panel sets. At t_0, just after the event, the system experiences a sharp decline from its nominal performance P_0 to P_1, resulting in a 40% reduction in total power flow. Hence, maintenance begins at t_1, after the breakdown has been detected and identified. The performance remains at the reduced level P_1 throughout the maintenance processing phase. Thus, optimized maintenance, displayed as the blue-colored line in Figure 15, ends at t_2, resulting in faster recovery of the system to its nominal performance. Standard maintenance processing, displayed as the red-colored line, takes longer and ends at t_3, delaying full system recovery.

Scenario 4. In Scenario 4, the restoration sequence and the performance drop are handled according to the following stages: At time t_0, the system experiences a major breakdown, causing a 100% performance drop, from nominal performance P_0 to 0% performance P_1. After the breakdown, the time between t_0 and t_1 is the time required to detect and identify the faults. In this scenario, according to the safety and security requirements on the one hand and to the order of reliability importance of the broken-down components on the other, the switch must be fixed first and then the inverter, before the PV panel sets. Both maintenance processes (standard and optimized) begin at time t_1. The optimized maintenance process restores the switch at t_2, which brings the system resilient performance back up to 60% performance P_2, as depicted in Figure 16, while the standard maintenance process restores the switch later at t_3, causing a delay in the system's recovery performance to 60%. The remaining components, specifically the inverter and then the sets of panels, are restored next. In the optimized maintenance process, the system's full performance

is achieved at time t_4. In the standard maintenance process, the system's full recovery happens later, at time t_5, resulting in prolonged downtime.

In Scenarios 1 and 2, the total time is determined primarily by the panel-set maintenance times. In Scenarios 3 and 4, the total time is determined by the inverter maintenance time, since it takes longer than the other components, with some contribution from the switch in Scenario 4.

Figure 14. Scenario 2 simulation: 2 sets of panels.

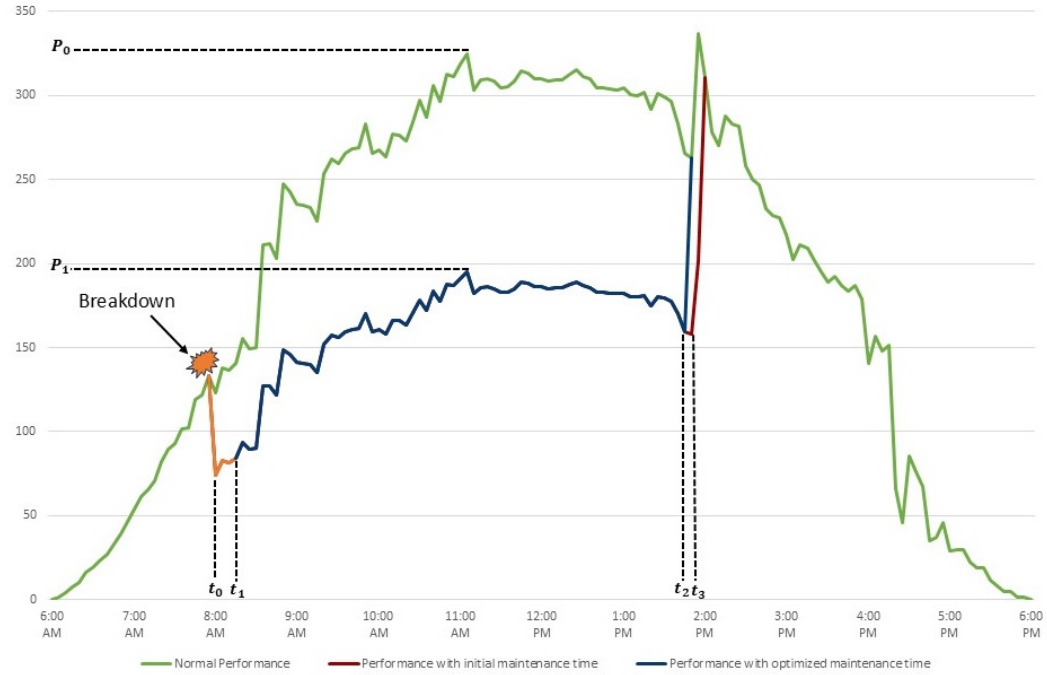

Figure 15. Scenario 3 simulation: sets of panels + inverter.

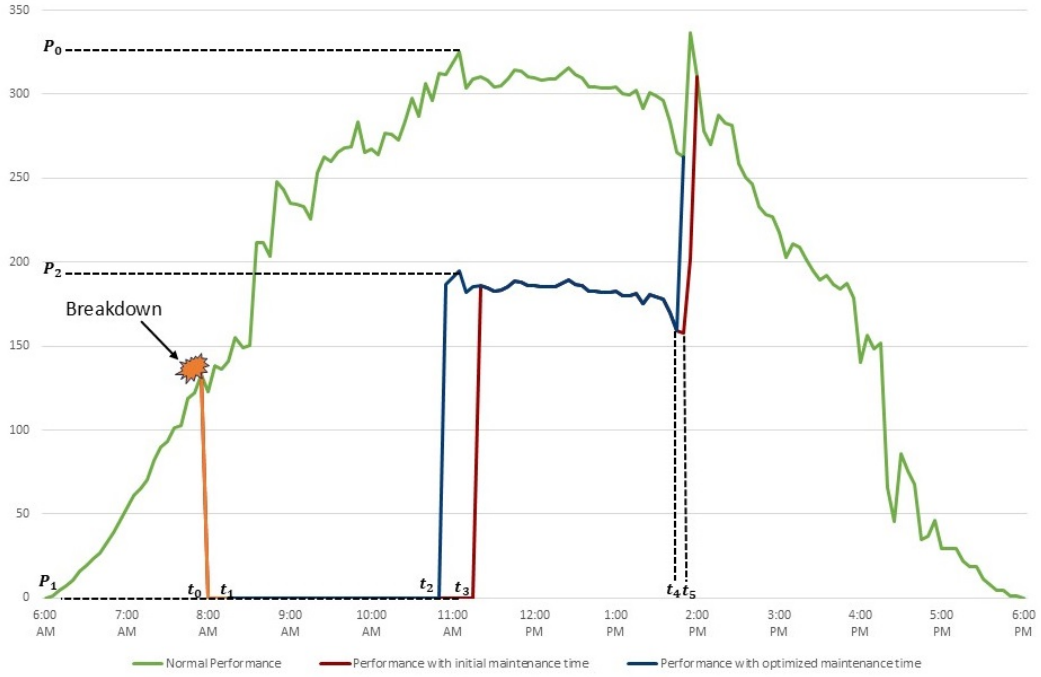

Figure 16. Scenario 4 simulation: sets of panels + inverter + switch.

5. Discussion

In the case study above, in the microgrid environment comprehensively covered by a sensor network, we can acquire precise and real-time data and information about equipment health status and environmental conditions. Nevertheless, even with such an efficient data collection system in place, uncertainties in data and prediction outcomes persist. To effectively quantify and address these issues, we employ risk Monte Carlo simulation techniques for decision risk assessment. In the first decision-making process, we innovatively integrate the risk function into a multi-objective optimization framework, enabling us to solve the problem for an optimal solution set while considering risk factors.

When progressing to the second decision-making process, we further translate risk factors into a specific metric of repair time and seamlessly integrate it as a crucial component of the sole objective function. This approach precisely guides the decision-making process, ensuring both the practicality and robustness of the decision outcomes.

Recovery time is minimized with our proposed model. This improvement, as shown by the reductions in Table 9, demonstrates the model's capability to allocate maintenance resources efficiently and prioritize repairs based on the criticality and failure probabilities of each component, ultimately ensuring a more robust and resilient microgrid system. For the set of PV panels, the initial maintenance time was 4.25 h. After optimization, this time was reduced to 3.88 h. The optimized schedule effectively decreases the maintenance duration for the PV panel set by 0.37 h, which is a reduction of approximately 8.7%. This decrease shortens the period during which the PV panels operate at reduced performance, thus enhancing the overall energy output. For the inverter, the initial maintenance time was 5.62 h, and the optimized time was 5.49 h. Although this reduction is smaller, 0.13 h (or about 2.3%), it remains significant due to the inverter's critical role in power conversion and system stability. For the switch, the initial maintenance time was 2.91 h, which was reduced to 2.5 h after optimization. This represents a reduction of 0.41 h, or 14.1%. Since the switch is essential to managing power flow, this reduction is particularly beneficial, as it enables quicker restoration of the system's connectivity and operational capacity. The reductions in maintenance times across these components highlight the precision and efficiency of the proposed decision-making model. By minimizing the time required to restore each component, the model not only reduces system downtime but also enhances resilience by allowing for quicker recovery after disruptions. This is particularly beneficial in critical

energy infrastructures where rapid response times are essential to maintaining stability and availability. The optimized maintenance times for these components translate into a cumulative decrease in overall repair duration, allowing the microgrid to return to full operational performance faster than with the traditional scheduling approach.

Table 9. Maintenance times per scenario.

Scenario	Failed Elements	Standard Repair Time	Optimized Repair Time	Stand. Total Repair Time	Optim. Total Repair Time
1	1 PV sets	4.25 h	3.88 h	4.25 h	3.88 h
2	2 PV sets	4.25 h	3.88 h	4.25 h	3.88 h
3	2 PV sets	4.25 h	3.88 h	5.62 h	5.49 h
	1 inverter	5.62h	5.49 h		
4	2 PV sets	4.25 h	3.88 h	5.62 h	5.49 h
	1 inverter	5.62 h	5.49 h		
	1 switch	2.91 h	2.50 h		

5.1. Contributions to Microgrid Resilience

As shown in Figure 17, with IoT-based predictive maintenance and risk-based decision making with uncertain information, the green curve presents a much lower degradation rate of system resilient performance, which drops to $L_3 > L_2$, with a shorter diagnosis time from t_2 to $t_3^{'}$ and a shorter time of repair $t_3^{'}$ to $t_4^{'}$.

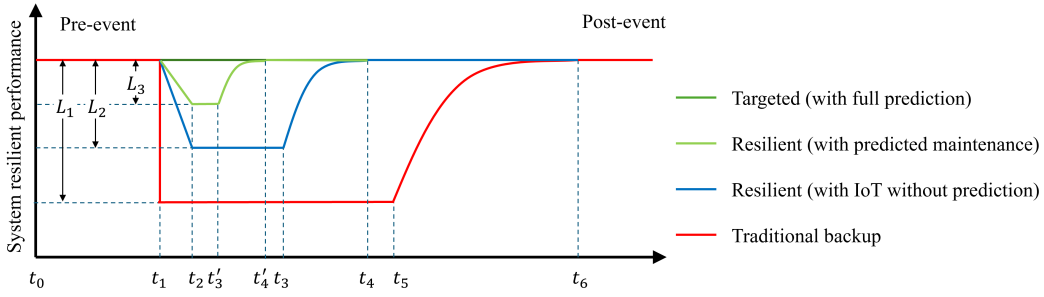

Figure 17. Resilient progress with risk-based predictive maintenance decisions.

First, this method reduces the recovery time and the duration of maintenance actions, thanks to a substantial enhancement in the system's ability to be maintained in operational conditions despite its components' failures. This ability, called maintainability, is defined by the European Committee for Standardization [37] as "the ability of an item, under given conditions of operation, to be retained in or restored to a state in which it can perform a required function when the maintenance activity is performed by qualified personnel using stated procedures and resources". Second, by utilizing the prediction capabilities, it becomes easier to plan maintenance tasks proactively. This means that one can anticipate which task needs to be performed and in which order during activities for recovery, allowing for saving both time and money. Reducing the time required to address issues and efficiently managing spare parts for repairs can prevent delays caused by waiting for parts to be ordered and delivered, which translates into system downtime reduction and cost savings. Additionally, system resilient performance improves, as maintenance actions can be scheduled more effectively, particularly with a large number of tasks as it happens after disastrous events. With a comprehensive overview of potential faults through IoT monitoring, multiple maintenance tasks can be coordinated, further optimizing operations and minimizing disruptions. In summary, saving time ultimately saves money, and proactive maintenance planning enhances overall system resilient performance.

5.2. Computational Requirements

The volume of data and computation needs for real-time risk assessment naturally escalate significantly with the scale of the sensor network.

In case 1, we performed Pareto optimization on a Lenovo ThinkPad X1 Extreme 2nd Gen laptop (manufactured by Lenovo, Shenzhen, China), equipped with an Intel Core i9-9880H processor (six cores at 2.3 GHz base frequency) and 16 GB memory. The entire computation took approximately 15 s on average for optimization using a multi-objective genetic algorithm, coded with the Python 3.9 programming language in the Windows 10 experimental environment. Given the small-scale problem, a limited number of production lines, and relatively simplified cost and risk models, the overall runtime was short despite the Monte Carlo simulation used in risk calculation, as it employed a simplified sampling method with a low number of simulations.

Our experience shows that within a localized scope, the computational time required is not exceptionally high for the real-time assessment of a specific risk. However, when evaluating the evolution and propagation of disastrous event effects within complex systems, the demand for computational power increases substantially.

From the perspective of real-time capability, "real-time" implies completing the assessment within the time frame required by the scenario. For real-time decision making, it is first essential to define the time constraints for "real-time" assessment. In practical engineering projects, thresholds are usually set for critical risk indicators to promptly halt the propagation of disasters or incidents within the system. In the case of large-scale disastrous events, early warning information is typically available days in advance, allowing for ample time to assess its impact on the system.

In a process of multi-sensor-based data-driven decision making, decision information fusion can be categorized into three levels: data-fusion level, feature-fusion level, and decision-fusion level. For large-scale scenarios, distributed data processing devices at the edge can be employed to preprocess data, extracting and transmitting key features or preliminary decision results to the system-level decision module. This approach reduces the data processing load at the system decision support level and enhances response efficiency. Such edge computing methods effectively alleviate the pressure on centralized data processing and enable distributed collaborative optimization.

If there is indeed a situation requiring the processing of a large number of data within a short period, typical operating conditions and risk datasets can be constructed in advance through simulation based on digital twin models, allowing on-site data to be matched with the dataset information to approximate real-time problem solving.

6. Conclusions

This study proposes a comprehensive framework that enhances the resilience of microgrids in the face of uncertainties and unexpected events by integrating sensor network-based monitoring and risk assessment-based decision support. The framework incorporates various information uncertainties in the decision-making processes of energy distribution and predictive maintenance and has been validated by using a real-world microgrid case in Ghana. The case study provides a detailed demonstration of the decision-making processes in different risk scenarios, proving the practical applicability and effectiveness of this approach.

This approach is equally applicable to power systems, railway systems [38], and other networked systems such as smart cities or smart buildings [39], with the core focus on utilizing IoT technology for data collection and the modeling of operating conditions and equipment–system interactions to enhance system resilience.

Before applying this method, it is essential to identify key decisions within the system throughout its different operating conditions, determine the components most critical to the system's resilience, recognize significant external events that could affect resilience, and quantify the risks related to potential decision-making errors. These requirements can guide specific data collection to construct a quantitative risk model.

When the monitored information and prediction results are uncertain, studies can be performed by using Monte Carlo simulation-type methods. Additionally, risk factors are incorporated into decision making, enhancing the system's resilience and responsiveness across different risk events.

In our case study, the number of sensors and risk factors is relatively low, primarily serving to illustrate the approach proposed in this paper. In real-world scenarios with a greater number of sensors, a large number of components and particularly the safety devices involved in the system typically require monitoring. In the case of highly complex environments, information extraction and risk assessment can be achieved in a hierarchical approach. For instance, when more data need to be collected, edge computing devices can preprocess the acquired signals at the sensor or local level, uploading only key features or results to the system decision-making layer. This approach effectively reduces the data processing load at the system level.

Future research will focus on extending and refining this framework to handle more complex decision-making scenarios, such as developing decision risk assessment models for intricate situations and exploring the propagation paths of risks related to the real-time assessment of components' *p-FV* reliability importance subject to data uncertainties within the system and their impact on microgrid stability. These studies will further enhance the adaptive capacity of microgrids in dynamic environments, providing more comprehensive support for risk management in distributed power systems.

Author Contributions: Conceptualization, K.H.A.; methodology, T.Y., K.R.A. and K.H.A.; software, T.Y. and K.R.A.; validation, T.Y. and K.R.A.; formal analysis, T.Y., K.R.A. and K.H.A.; investigation, T.Y. and K.R.A.; resources, K.H.A. and H.W.; data curation, T.Y. and K.R.A.; writing—original draft preparation, T.Y. and K.R.A.; writing—review and editing, K.H.A., A.S.A.A. and H.W.; visualization, T.Y., K.R.A. and K.H.A.; supervision, K.H.A., A.S.A.A. and H.W.; project administration, K.H.A., A.S.A.A. and H.W.; funding acquisition, A.S.A.A. and K.H.A. All authors have read and agreed to the published version of the manuscript.

Funding: This research was funded by the Foreign Experts Recruitment Plan of China, and World Bank through CERME (Centre d'Excellence Régional pour la Maîtrise de l'Electricité).

Data Availability Statement: All data included in this study are available upon reasonable request by contacting the corresponding author.

Conflicts of Interest: The authors declare no conflicts of interest.

References

1. Ustun, T.S.; Ozansoy, C.; Zayegh, A. Recent developments in microgrids and example cases around the world—A review. *Renew. Sustain. Energy Rev.* **2011**, *15*, 4030–4041.
2. Patrao, I.; Figueres, E.; Garcerá, G.; González-Medina, R. Microgrid architectures for low voltage distributed generation. *Renew. Sustain. Energy Rev.* **2015**, *43*, 415–424.
3. Qiao, L.; Vincent, R.; Ait-Ahmed, M.; Tianhao, T. Microgrid Modeling Approaches for Information and Energy Fluxes Management based on PSO. In Proceedings of the 16th International Conference on Informatics in Control, Automation and Robotics, Prague, Czech Republic, 29–31 July 2019; pp. 220–227.
4. Dubois, A.M.; Badosa, J.; Calderón-Obaldía, F.; Atlan, O.; Bourdin, V.; Pavlov, M.; Young Kim, D.; Bonnassieux, Y. Step-by-step evaluation of photovoltaic module performance related to outdoor parameters: Evaluation of the uncertainty. In Proceedings of the 2017 IEEE 44th Photovoltaic Specialist Conference (PVSC), Washington, DC, USA, 25–30 June 2017; pp. 626–631.
5. Smith, A.; Katz, R. Us billion-dollar weather and climate disasters: Data sources, trends, accuracy and biases. *Nat. Hazards* **2013**, *67*, 387–410.
6. Staudt, A.; Curry, R. *More Extreme Weather and the us Energy Infrastructure*; National Wildlife Federation Report 16; National Wildlife Federation: Reston, VA, USA, 2011. Available online: https://www.epa.gov/sites/default/files/documents/final_nwf_energyinfrastructurereport_4-8-11.pdf (accessed on 11 October 2024).
7. Panteli, M.; Mancarella, P. Modeling and Evaluating the Resilience of Critical Electrical Power Infrastructure to Extreme Weather Events. *IEEE Syst. J.* **2017**, *11*, 1733–1742.
8. Zhaohong, B.; Yanling, L.; Gengfeng, L.; and Furong, L. Battling the extreme: A study on the power system resilience. *Proc. IEEE* **2017**, *105*, 1253–1266.

9. Tuna, G.; Gungor, V.C.; Gulez, K. Wireless Sensor Networks for Smart Grid Applications: A Case Study on Link Reliability and Node Lifetime Evaluations in Power Distribution Systems. *Int. J. Distrib. Sens. Networks*, **2013**, *9*, 796248.
10. Fadel, E.; Gungor, V.C.; Nassef, L.; Akkari, N.; Malik, M.G.A.; Almasri, S.; Akyildiz, I.F. A Survey on Wireless Sensor Networks for Smart Grid. *Comput. Commun.* **2015**, *71*, 22–33.
11. Dui, H.; Li, H.; Dong, X.; Wu, S. An Energy IoT-Driven Multi-Dimension Resilience Methodology of Smart Microgrids. *Reliab. Eng. Syst. Saf.* **2025**, *253*, 110533.
12. *United States Air Force Risk Management (RM) Guidelines and Tools*; Department of the Air Force Department of the Air Force: Arlington County, VA, USA, 2022.
13. Wang, Y.; Rousis, A.O.; Strbac, G. On Microgrids and Resilience: A Comprehensive Review on Modeling and Operational Strategies.*Renew. Sustain. Energy Rev.* **2020**, *134*, 110313.
14. Mishra, S.; Anderson, K.; Miller, B.; Boyer, K.; Warren, A. Microgrid Resilience: A Holistic Approach for Assessing Threats, Identifying Vulnerabilities, and Designing Corresponding Mitigation Strategies. *Appl. Energy* **2020**, *264*, 114726.
15. Hamidieh, M.; Ghassemi, M. Microgrids and Resilience: A Review. *IEEE Access* **2022**, *10*, 106059–106080.
16. Panteli, M.; Pickering, C.; Wilkinson, S.; Dawson, R.; Mancarella, P. Power System Resilience to Extreme Weather: Fragility Modeling, Probabilistic Impact Assessment, and Adaptation Measures. *IEEE Trans. Power Syst.* **2017**, *32*, 3747–3757.
17. Kaloti, S.A.; Chowdhury, B.H. Toward Reaching a Consensus on the Concept of Power System Resilience: Definitions, Assessment Frameworks, and Metrics. *IEEE Access* **2023**, *11*, 81401–81418.
18. Leoni, L.; De Carlo, F.; Paltrinieri, N.; Sgarbossa, F.; BahooToroody, A. On risk-based maintenance: A comprehensive review of three approaches to track the impact of consequence modelling for predicting maintenance actions. *J. Loss Prev. Process Ind.* **2021**, *72*, 104555.
19. Abbassi, R.; Arzaghi, E.; Yazdi, M.; Aryai, V.; Garaniya, V.; Rahnamayiezekavat, P. Risk-based and predictive maintenance planning of engineering infrastructure: Existing quantitative techniques and future directions. *Process Saf. Environ. Prot.* **2022**, *165*, 776–790.
20. Arunraj, N.S.; Maiti, J. Risk-based maintenance: Techniques and applications. *J. Hazard. Mater.* **2007**, *142*, 653–661.
21. Khan, F.I.; Haddara, M. Risk-Based Maintenance (RBM): A new approach for process plant inspection and maintenance. *Process Saf. Prog.* **2004**, *23*, 252–265.
22. Brown, S.J.; May, I.L. Risk-based hazardous release protection and prevention by inspection and maintenance. *J. Pressure Vessel Technol.* **2000**, *122*, 362–367.
23. Wade, H. The Elephant in the Room, or the Impact of Measurement Uncertainty on Risk-ProQuest. *Quality* **2023**, *62*, 12.
24. *ISO/IEC 25024:2015(E)*; Software Engineering—Software Product Quality Requirements and Evaluation (SQuaRE)—Data Quality Model. ISO: Geneva, Switzerland, 2015.
25. Kirchen, I.; Schutz, D.; Folmer, J.; Vogel-Heuser, B. Metrics for the Evaluation of Data Quality of Signal Data in Industrial Processes. In Proceedings of the 2017 IEEE 15th International Conference on Industrial Informatics (INDIN), Emden, Germany, 24–26 July 2017; IEEE: Piscataway, NJ, USA, 2017; pp. 819–826.
26. Liao, R.; He, Y., Feng; T., Yang, X.; Dai, W.; Zhang, W. Mission reliability-driven risk-based predictive maintenance approach of multistate manufacturing system. *Reliab. Eng. Syst. Saf.* **2023**, *236*, 109273.
27. Edwards, J.S.; Duan, Y.; Robins, P.C. An Analysis of Expert Systems for Business Decision Making at Different Levels and in Different Roles. *Eur. J. Inf. Syst.* **2000**, *9*, 36–46.
28. Duan, Y.; Edwards, J.S.; Dwivedi, Y.K. Artificial Intelligence for Decision Making in the Era of Big Data Evolution, Challenges and Research Agenda. *Int. J. Inf. Manage.* **2019**, *48*, 63–71.
29. Meng, X.; Zhu, J.; Chen, G.; Shi, J.; Li, T.; Song, G. Dynamic and Quantitative Risk Assessment under Uncertainty during Deepwater Managed Pressure Drilling. *J. Clean Prod.* **2022**, *334*, 130249.
30. Li, X.; Chen, D.; Fu, J.; Liu, S.; Geng, X. Construction and Application of Fuzzy Comprehensive Evaluation Model for Rockburst Based on Microseismic Monitoring. *Appl. Sci.* **2023**, *13*, 12013.
31. Sun, D.; Wang, H.; Huang, J.; Zhang, J.; Liu, G. Urban Road Waterlogging Risk Assessment Based on the Source?Pathway?Receptor Concept in Shenzhen, China. *J. Flood Risk Manag.* **2022**, *16*, e12873. https://doi.org/10.1111/jfr3.12873.
32. Liu, J.; Wang, D.; Lin, Q.; Deng, M. Risk Assessment Based on FMEA Combining DEA and Cloud Model: A Case Application in Robot-Assisted Rehabilitation. *Expert Syst. Appl.* **2023**, *214*, 119119.
33. Adjallah, K.H.; Adzakpa, K.P. Minimizing maintenance cost involving flow-time and tardiness penalty with unequal release dates. *Proc. Inst. Mech. Eng. O* **2007**, *221*, 57–65.
34. Kuo, W.; Zhu, X. Relations and Generalizations of Importance Measures in Reliability. *IEEE Trans. Reliab.* **2012**, *61*, 659–674.
35. Kuo, W.; Zhu, X. *Importance Measures in Reliability, Risk, and Optimization: Principles and Applications*; John Wiley & Sons: Hoboken, NJ, USA, 2012; pp. 63–67.
36. International Atomic Energy Agency. *Generic Component Reliability Data for Research Reactor PSA*; IAEA-TECDOC-930; IAEA: Vienna, Austria, 1997.
37. *13306 CEN/TC 319EN*; Maintenance—Maintenance Terminology. European Standard, Bruxelles, Belgium, 2010.

38. Chen, J.; Hu, H.; Wang, M.; Ge, Y.; Wang, K.; Huang, Y.; Yang, K.; He, Z.; Xu, Z.; Li, Y.R. Power Flow Control-Based Regenerative Braking Energy Utilization in AC Electrified Railways: Review and Future Trends. *IEEE Trans. Intell. Transp. Syst.* **2024**, *25*, 6345–6365.
39. Song, Y.; Wan, C.; Hu, X.; Qin, H.; Lao, K. Resilient Power Grid for Smart City. *iEnergy* **2022**, *1*, 325–340.